



# LUND UNIVERSITY

## Laplace distribution models for road topography and roughness

Johannesson, Pär; Podgorski, Krzysztof; Rychlik, Igor

2015

[Link to publication](#)

*Citation for published version (APA):*

Johannesson, P., Podgorski, K., & Rychlik, I. (2015). *Laplace distribution models for road topography and roughness*. (Working Papers in Statistics; No. 14). Department of Statistics, Lund university.

*Total number of authors:*

3

### General rights

Unless other specific re-use rights are stated the following general rights apply:

Copyright and moral rights for the publications made accessible in the public portal are retained by the authors and/or other copyright owners and it is a condition of accessing publications that users recognise and abide by the legal requirements associated with these rights.

- Users may download and print one copy of any publication from the public portal for the purpose of private study or research.
- You may not further distribute the material or use it for any profit-making activity or commercial gain
- You may freely distribute the URL identifying the publication in the public portal

Read more about Creative commons licenses: <https://creativecommons.org/licenses/>

### Take down policy

If you believe that this document breaches copyright please contact us providing details, and we will remove access to the work immediately and investigate your claim.

LUND UNIVERSITY

PO Box 117  
221 00 Lund  
+46 46-222 00 00

Working Papers in Statistics  
No 2015:14

Department of Statistics  
School of Economics and Management  
Lund University

# Laplace distribution models for road topography and roughness

---

PÄR JOHANNESSON, SP TECHNICAL RESEARCH INSTITUTE OF SWEDEN

KRZYSZTOF PODGÓRSKI, LUND UNIVERSITY

IGOR RYCHLIK, CHALMERS UNIVERSITY OF TECHNOLOGY





# Laplace distribution models for road topography and roughness

PÄR JOHANNESSON\*, KRZYSZTOF PODGÓRSKI\*\*, IGOR RYCHLIK\*\*\*

## Addresses:

\* SP Technical Research Institute of Sweden, Box 24036, SE-400 22 Göteborg, Sweden  
Par.Johannesson@sp.se (Corresponding author)

\*\* Department of Statistics, Lunds University, SE-220 07 Lund, Sweden  
krzysztof.podgorski@stat.lu.se

\*\*\* Mathematical Sciences, Chalmers University of Technology, SE-412 96 Göteborg, Sweden  
rychlik@chalmers.se

**Abstract:** Gaussian models are frequently used for road profiles. However, these models are often only valid for short sections of the road. Here we present a comprehensive approach to describe various aspects of road surface/elevation by using extensions of Gaussian models arising from random gamma distributed variances. These random variances result in the Laplace distribution and thus we refer to the so defined models as Laplace models. The approach is shown to perform well in modelling road topography, road roughness and multi-valued responses of forces and bending moments containing transients. The different Laplace models are presented together with numerical examples and Matlab code for simulation.

**Keywords:** Road profile; topography; road roughness; generalized Laplace distribution; non-Gaussian process; autoregressive process; power spectral density (PSD); ISO spectrum; international roughness index (IRI); vehicle durability; fatigue damage.

## Biographical notes:

Pär Johannesson received his PhD in Mathematical Statistics in 1999 at Lund Institute of Technology, with a thesis on statistical load analysis for fatigue. He has published about 15 papers in international journals, and is a co-editor of the handbook *Guide to Load Analysis for Durability in Vehicle Engineering*. He is currently working as a researcher at SP Technical Research Institute of Sweden, mainly within industrial and research projects on statistical methods for load analysis, reliability and fatigue.

Krzysztof Podgórski is Professor in Statistics at Lund University. He earned his PhD in Statistics at Michigan State University in 1993, with the thesis entitled *Resampling methods for linear models*. He has published about 50 papers in peer reviewed journals in probability theory, statistics and applications and is a co-author of the monograph *The Laplace Distribution and Generalizations. A Revisit with New Applications*.

Igor Rychlik is Professor in Mathematical Statistics at Chalmers University of

Technology. He earned his PhD in 1986, with a thesis entitled *Statistical wave analysis with application to fatigue*. He has published more than 80 papers in international journals, is a co-author of the textbook *Probability and Risk Analysis. An Introduction for Engineers*.

## 1 Introduction

Durability assessment of vehicle components often requires a customer or market specific load description. It is therefore desirable to have a model of the load environment that is vehicle independent and which may include many factors: encountered road roughness, topographic characteristics such as hilliness and curvature, cargo loading, driver behaviour and legislation, see for example (Edlund & Fryk, 2004), for a description of the Global Transport Application (GTA). In the transportation engineering research, the road elevation variability is divided into three distinct components: topography, roughness and texture. Texture is made of the high frequency components responsible for noise, skid-resistance and tyre wear. Roughness is the road unevenness, containing wavelengths from about 0.1 m to 50 m, and cause vibration responses in the vehicle structure and components which may lead to fatigue problems. A continuous stochastic process modelling roughness is typically utilized to evaluate risks of fatigue failures. Topography is the low frequency part of the elevation, corresponding to landscape variability, and is one of the most important factors in fuel consumption of vehicles, as well as an important load input for fatigue assessment of transmission components.

Traditionally, road profiles on different scales have been modelled by using Gaussian processes; see e.g. (Dodds & Robson, 1973; ISO 8608, 1995; Andr n, 2006). However, it is well known that measured road profiles contain shorter segments with above average irregularity – the property that Gaussian distribution based models have difficulty to account for. Several approaches has been suggested to extend Gaussian modelling in order to capture this particular behaviour, see e.g. (Bogsj , 2007b; Charles, 1993; Bruscella et al., 1999; Rouillard, 2004, 2009) and the references therein. The road topography modelling is closely related to simulation of vehicle missions and definition of stochastic drive cycle profiles for evaluation of fuel consumption, see e.g. (Souffran et al., 2012; Schwarzer et al., 2010). In this work, we discuss a novel approach, based on the Laplace distribution, to model roughness and topography of road profiles. We do not discuss texture modelling as the potential of our approach for this purpose is yet to be investigated.

In simple terms, the proposed modelling is a modification of Gaussian modelling in which variances are becoming random. For example, for a Gaussian time series  $X_k$  one can introduce a simple extension by scaling it independently of  $X_k$  by gamma distributed random scaling factors  $\sqrt{R_k}$ . A new time series  $Y_k = \sqrt{R_k}X_k$ , which is Laplace distributed, shows entirely new qualities not observed in its Gaussian counterpart. Its distinctive properties have been proven

useful in many areas in engineering, ecology, and finance, see (Kotz et al., 2001; Kozubowski et al., 2013) for a theoretical background. Here we demonstrate the applicability of this approach to road surface modelling. Both time series and continuous process signals are considered for topography and roughness, respectively. Our study shows that the Laplace model has the flexibility in describing both continuous and discrete time data, extensions to multivariate tracks, and easiness of fitting to the real data. Most importantly and in contrast to the Gaussian case, it has the ability to account for transients and other sudden road irregularities, which is often observed in road surface data and thus is essential for fatigue assessment.

### **Topography**

Road topography is often described using slopes of hills observed in the records, which are discrete time series. In the measured topography data, it is often observed that variability of the slopes appears to be local, i.e. periods of high variability are followed by the ones with much smaller variability. This brings the model of the form  $Y_k = \sqrt{R_k}X_k$  for the slopes as a natural candidate to capture the locality of variance. The model has two additional parameters in order to describe local variability of variance. Once the model is fitted to the data it can be utilized in dedicated programs to simulate fuel consumption of vehicles as well as to estimate energy losses. In fact, the presented study was initiated by investigations of efficiency of different technical solutions to harvest energy from breaking and driving downhill of utility vehicles in mines, see (Johannesson et al., 2015b). The empirical example that is used in this paper to illustrate the proposed model is based on topography records from a road surface segment in a mine.

### **Roughness**

We consider modelling of the road surface roughness with focus on durability applications. The most desired properties of the models are robustness and simplicity, so that only a small number of parameters need to be used to describe and classify homogeneous parts of the road. It is also of interest to reconstruct road profiles based on roughness measurements, e.g. the so-called International Roughness Index (IRI), which is often available from road administration databases.

Traditionally, roughness data are modelled by a Gaussian moving average, i.e. filtered (smoothed) Gaussian noise  $X_k$ . In (Bogsjö et al., 2012) it was shown that replacing Gaussian noise by Laplace noise  $\sqrt{R_k}X_k$  produces a more accurate model of roughness. In this paper we summarize principles of Laplace distribution modelling that arise from work in (Åberg et al., 2009; Bogsjö et al., 2012) and its extensions and applications presented in (Johannesson & Rychlik, 2013, 2014; Kvanström et al., 2013; Johannesson et al., 2015a; Kozubowski et al., 2013).

### **Multi-dimensional loads**

Considering just a single path along the road may be not sufficient for some applications, as any four-wheeled vehicle is subjected to excitations due to road roughness in the left as well as the right wheel paths. Clearly, two-tracks data are strongly correlated, particularly in the regions of high roughness of the roads. Here we give extensions of the Laplace models to multiple correlated signals to cover the case of road profiles along parallel tracks, see (Kozubowski et al., 2013; Johannesson et al., 2015a).

Multivariate Laplace model are also used in situation in which one has to account in multivariate signals for transients that have a common origin, for example, vibrations that can be caused by large obstacles encountered by a vehicle driving into potholes. Here we illustrate it to model forces and bending moment in a cultivator frame, see (Kvanström et al., 2013).

### **Structure of paper**

The paper is organized as follows. Road topography modelling is discussed in Section 2. In Section 3, the road roughness model is presented, while Section 4 is devoted to multivariate extensions. The paper closes with conclusions that address specifically each of the three main sections, acknowledgments, references and four appendixes. In the first appendix some details on simulation of the AR(1) Laplace model for topography are given, in the second one means to simulate Laplace roughness models are presented, an algorithm and MATLAB code to simulate the Laplace model for parallel road profiles are given in the third appendix. Finally, in the fourth appendix an algorithm to simulate the multi-valued Laplace load is presented.

## **2 Road topography modelling**

The task has been to develop a stochastic model for the topography to be used for fuel consumption evaluation and for life prediction of e.g. transmission components. The topography is the slope encountered by a vehicle due to the landscape variability. The encountered topography can be obtained from map and/or satellite data or by measurement systems on vehicles. For vehicle manufacturers it is desirable to be able to calculate the topography and its model parameters based on data available from the on-board logging system. In such a case, the extracted topography parameters could be stored on-board the vehicle in a compact format, which enables to collect statistics from a large fleet of vehicles. Therefore, it is of interest that the models are as simple as possible, but still being able to capture the main features of the topography.

## 2.1 Example of topography data

The data of encountered topography has been obtained using the on-board logging system of the articulated hauler. More precisely, the slope has been calculated based on the measured vehicle inclination which is corrected for the vehicle accelerations. The topography is usually defined as wavelengths of 50 metres and above, whereas wavelengths from 10 cm up to 50 metres are classified as road roughness. Therefore, in order to get the topography, the average value of the slope for each 25 metre segment is calculated. This will act as a low pass filter of the signal. The result is the 'measured' topography signal  $y(x)$ , as function of the distance  $x$ , with sampling distance of  $L_s = 25$  metres, see Figure 1. The topography signal can be converted to the altitude,  $z(x)$ , as function of distance.

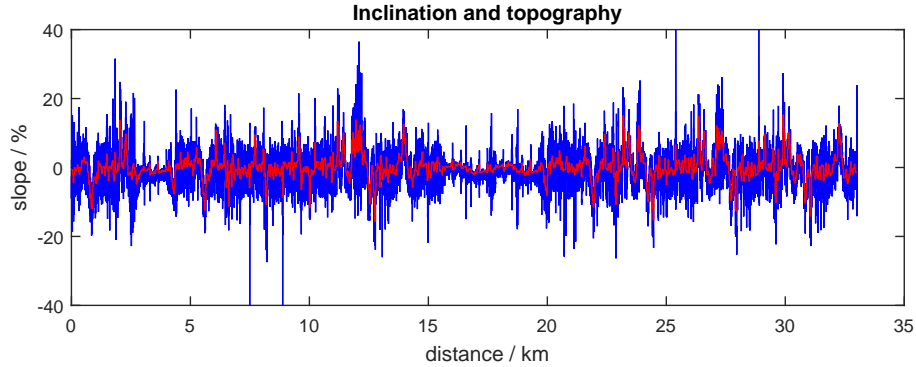


Figure 1: Measured slope and calculated topography for sampling distance of  $L_s = 25$  metres.

## 2.2 The Gaussian model of topography

The aim now is to find a simple but still useful model for the topography signal,  $y_k$ , here sampled with sampling distance  $L_s = 25$  m. We propose to model the topography  $Y_k$  by an autoregressive model, namely an AR(1)-model with only one regression parameter  $a$ , mean  $m$  and scale parameter  $\sigma_y$ , defined as

$$Y_k = \sigma_y X_k + m, \quad (1)$$

where  $X_k$  is a standardized Gaussian AR(1)-process, namely

$$X_k = a X_{k-1} + \sqrt{1 - a^2} e_k, \quad (2)$$

where  $e_k$  is modelled as independent normal random variables with expectation zero and variance one. The mean  $m$  is assumed to be zero unless otherwise stated. Note that the parameter  $\sigma_y$  is the standard deviation of the topography, i.e. a measure of the severity of the topography, whereas the regression parameter  $a$  is the

one-step correlation that indicates how fast the topography changes; a value close to one indicates a slowly varying topography, while a lower value indicates a faster varying topography with more smaller hills up and down. In fact, the mean length of a hill can be calculated from  $a$

$$L_{hill} = \frac{1}{\frac{1}{4} - \frac{1}{2\pi} \arcsin a} \cdot L_s \quad (3)$$

giving 700 metres for  $a = 0.9$  and 340 metres for  $a = 0.6$ .

### 2.3 Estimation

There are different methods to estimate the parameters of AR-processes. Here, we present the standard correlation method and an alternative approach called the zero-crossing method.

#### Correlation method

The parameter  $a$  is easily estimated, as well as the variance  $\sigma_y^2$ . The correlation method, which is the same as the Yule-Walker method, preserves the observed variance and one-step correlation of the signal. The parameters are then estimated as

$$\hat{a} = r_1/r_0 \quad (4)$$

$$\hat{\sigma}_y^2 = r_0 \quad (5)$$

where  $r_0$  is the sample variance and  $r_1$  the sample one-step covariance. The estimated AR-parameters for the measured topography can be used to characterize the topography of the measurement; for the signal we get ( $a = 0.734, \sigma_y = 3.71$ ).

#### Zero-crossing method

Another way to estimate the correlation  $a$  is to utilize an important characteristic of the time series of slopes - the frequency of encountered hills  $f$  (in the sampling frequency unit), defined as follows. The number of encountered hills is the number of times that the slope signal up-crosses level zero. Thus, the frequency of hills is equal to the frequency of zero upcrossings in the Gaussian time-series  $X_k$ . Now, for a zero mean stationary and ergodic Gaussian time series, the frequency of zero upcrossings is given by

$$f = P(X_1 < 0, X_2 > 0) = \frac{1}{4} - \frac{1}{2\pi} \arcsin a. \quad (6)$$

By counting the number of upcrossings in the topography signal, the observed frequency  $\hat{f}$  can be used to estimate the correlation parameter, namely

$$\hat{a} = -\sin(2\pi(\hat{f} - 1/4)) \quad (7)$$

$$\hat{\sigma}_y^2 = r_0 \quad (8)$$

and for the example signal we get ( $a = 0.755, \sigma_y = 3.71$ ).

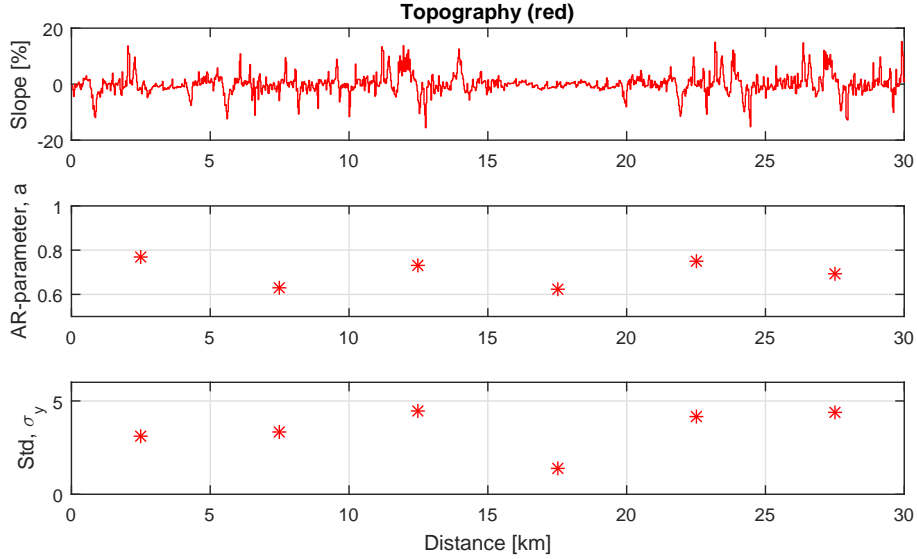


Figure 2: Above: Measured slope and calculated topography for sampling distance of  $L_s = 25$  metres. Below: Estimated AR-parameters for 5 km sections.

### Splitting into section

For long measurements, the characteristics of the topography are expected to change over time. Therefore, having the same AR-parameters for the complete measurement may not be appropriate. One approach is then to split the measurement into sections of, say, 5 km, and estimate AR-parameters ( $\hat{a}$ ,  $\hat{\sigma}_y$ ) for each 5 km section of the measured topography  $y_k$ . The topography of the measurement is then characterized by a sequence of AR-parameters. This is shown in the Figure 2, where we can observe that the AR-parameters are varying, with the fourth section having smaller  $\sigma_y$  and the  $a$ -parameter varying from 0.6 to 0.8.

## 2.4 The Laplace autoregressive model for topography

We have previously proposed to model the topography  $y_k$  by a Gaussian autoregressive model. However, the distribution of the topography does not always agree very well with the Gaussian one, see Figure 3. We will here describe how the Gaussian AR-model can be extended, by constructing a so-called Laplace AR-process. We will illustrate it with a measurement from Jaro, see Figure 1. The complete measurement of 33 km will be modelled as a stationary signal, which looks reasonable in this case.

A Laplace random variable can be constructed as the product

$$Y = \sigma_y \sqrt{R} X + m, \quad (9)$$

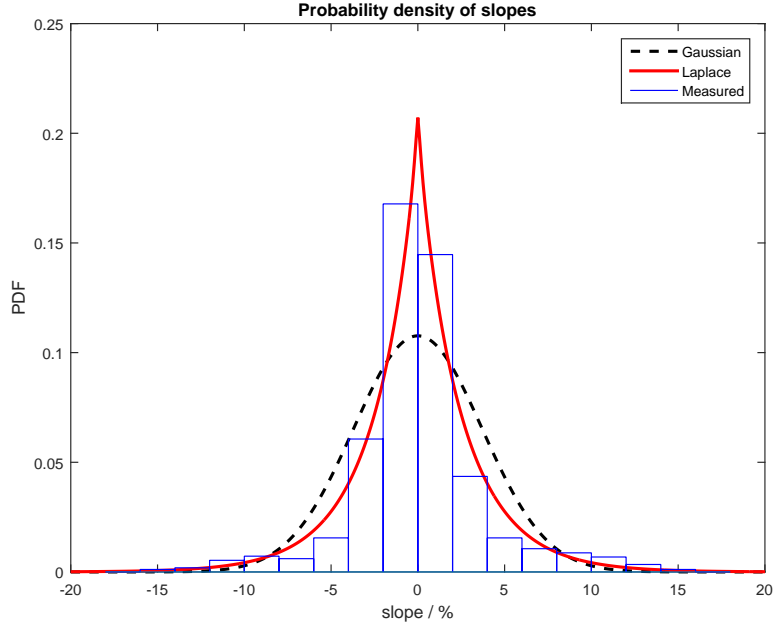


Figure 3: Normalized histogram of measured topography compared with Gaussian (dashed line) and Laplace (red solid line) distributions.

where  $X$  is normally distributed with mean zero and variance one, and  $R$  is gamma distributed with mean one and variance  $\nu$ , having the following probability density function

$$f(r) = \frac{1}{\Gamma(1/\nu)\nu^{1/\nu}} r^{1/\nu-1} \exp(-r/\nu), \quad (10)$$

where  $\Gamma(\cdot)$  is the gamma function. Note that if the parameter  $\nu = 0$ ,  $Y$  becomes the Gaussian case. The standard deviation  $\sigma_y$  is estimated from the signal, and the parameter  $\nu$  is estimated through the kurtosis  $\kappa$  of the signal,  $\nu = (\kappa - 3)/3$ . The estimated parameters for the 33 km long Jaro signal are  $\sigma_y = 3.71$  and  $\nu = 1.11$ . In Figure 3 the normalized histogram of observed data is compared to the estimated PDFs of Gaussian and Laplace distributions. We observe that the Laplace distribution gives a much better fit compared to the Gaussian one.

We will now describe how the Gaussian AR-model can be extended, by constructing the so-called Laplace AR-process as an amplitude-modulated Gaussian AR-process

$$Y_k = \sigma_y \sqrt{R_k} X_k + m \quad (11)$$

where  $X_k$ 's follow the Gaussian AR(1), see Eq. (2), while  $R_k$ 's are gamma random variables with mean one and variance  $\nu$ , independent of  $X_k$ 's. A simulation example with independent gamma variables is shown in Figure 4, with parameters  $a = 0.734$ ,  $\sigma_y = 3.71$  and  $\nu = 1.11$  corresponding to the Jaro signal. The upper graph shows the Gaussian AR-process, the middle one the square root of the

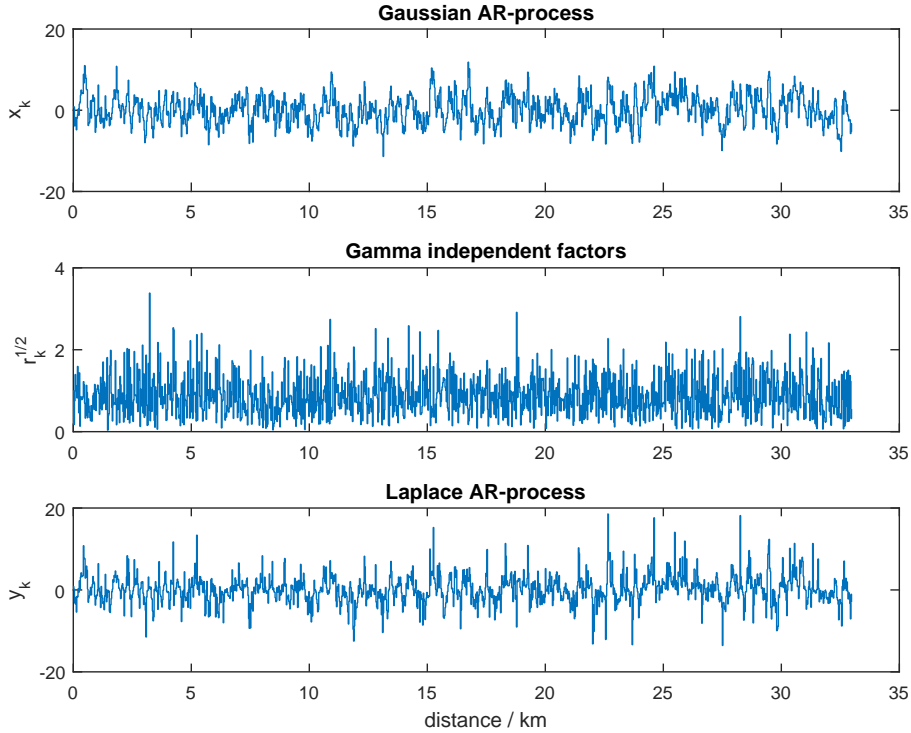


Figure 4: Simulated Laplace AR-process with independent gamma variables.

gamma variables, and the lower one the Laplace AR-process.

### Laplace model with correlated variances

In this section we present a model for correlated factors  $R_k$ . The simplest Laplace model is obtained by assuming that the factors  $R_k$  are independent. Then, the Laplace AR-model can be described by one extra parameter  $\nu$ , compared to the Gaussian AR-model. It seems reasonable to believe that the variance of the topography varies slowly, and hence the factors  $R_k$  are likely dependent between themselves. The degree of dependence is a function of the chosen length of the constant variance segments (here 25 metres). In (Johannesson et al., 2015b) an autoregressive model for the normalized variances  $R_k$  was suggested. The model has one regression parameter  $a_r$ , and it can be shown that it has exponentially decaying autocorrelation  $a_r^k$ ,  $k = 0, 1, \dots$ , see (Sim, 1971), where the gamma autoregressive model has been introduced, or (Kozubowski & Podgórski, 2008), where a historical overview and further properties of this model are presented.

More details on the gamma AR(1) model is presented in Appendix A.1 together with Matlab code for simulation of a Laplace AR-model. A simulation example with correlated gamma variables is shown in Figure 5, where the parameters correspond to the Jaro signal;  $a = 0.734$ ,  $\sigma_y = 3.71$ ,  $\nu = 1.11$  and  $a_r = 0.84$ .

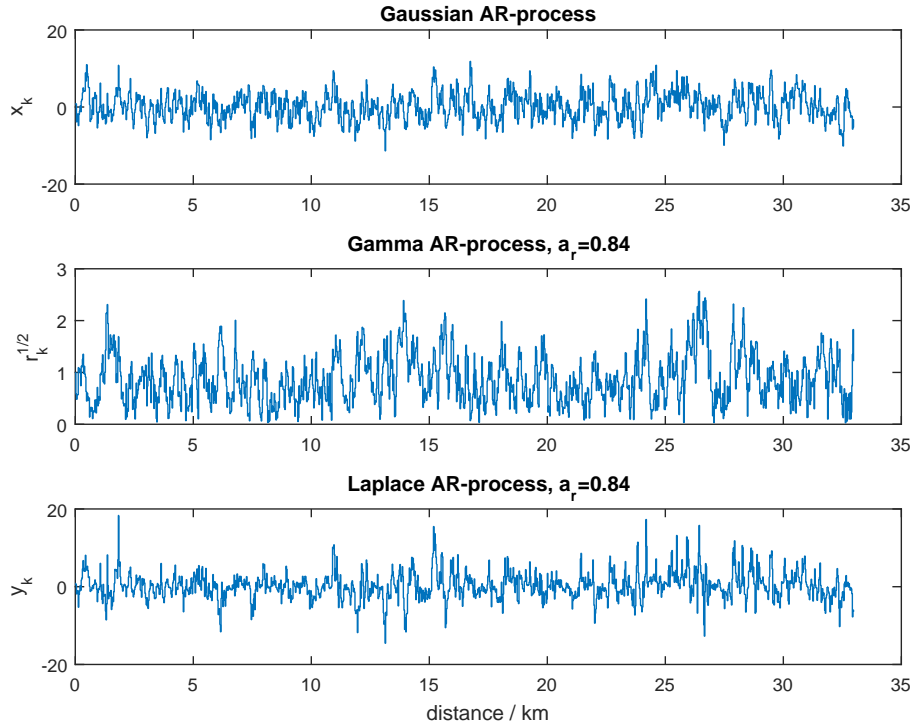


Figure 5: Simulated Laplace AR-process with correlated gamma variables.

## 2.5 Validation with respect to fuel consumption

Evaluation of fuel efficiency is important and needs to be understood in early project phases, since it is an important part of the total cost of ownership. Thus, the variability of the operating environment needs to be characterized, as well as the variation between customers. One of the most important sources of variation in fuel consumption is topography.

The task here is to study the variation in the fuel consumption for stochastically generated topographies. The fuel consumption is simulated with a vehicle simulation model of a construction machine implemented in Simulink. With a given topography, the model simulates driving the vehicle using a detailed model of the engine and transmission. Both the measured topography and generated ones using the autoregressive modelling technique have been used as input to the simulation model. Here measurements from the Jaro site are analysed. The topography that is measured originates from a track that starts and ends at the same point (consequently also at the same height). Despite this, the measured topographies feature a steady descent giving a difference between the start and end heights, implicating that there is a bias in the measurements. This is amended by a correction that subtracts the average slope from the measured topography to form a corrected topography with zero accumulated height change. The simulated accumulated fuel consumptions as function of distance for these topographies are shown in Fig-

ure 6(left).

Fuel consumptions are also presented for five topographies generated using the AR model with parameters estimated from the measured topography (the measured and corrected topographies give equal estimation of parameters). The variant of the AR modelling used for generating the topographies is of the Gaussian type. An alternative variant, the Laplace type which is not shown here, gives quantitatively similar results. In Figure 6(right) the total consumed fuel at the end of the track is given for 25 generated topographies, together with their estimated mean and one-standard-deviations. The total consumed fuel for the measured and corrected topographies are also given. It is seen that the measured original topology gives 20% lower fuel consumptions compared to the corrected one, which is a consequence of the artificial downhill slope due to the bias. The corrected measured topography instead comes very close to the mean of the generated topographies, indicating that the generated topographies are good descriptions for evaluating simulated fuel consumption. The relative standard deviation in the simulated fuel consumption, due to stochastically generated topographies, is about 5%. Most of this variation is due to difference in start and end altitude. If the generated topographies are adjusted to have the same start end altitude, the variation in fuel consumption drops to about 1%.

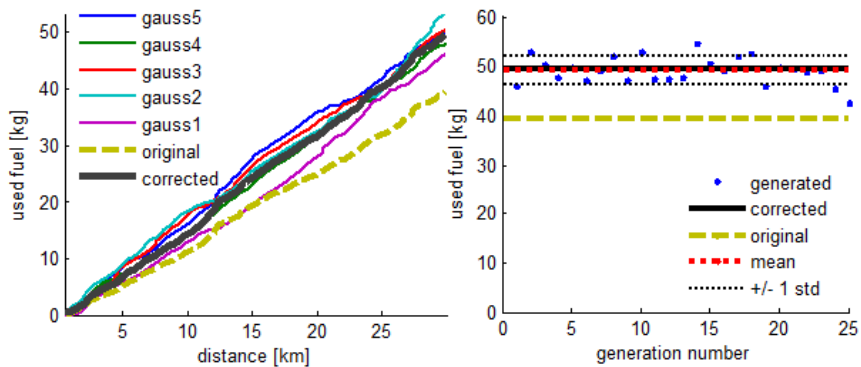


Figure 6: (left) Used fuel along the track for generated and measured topographies. (right) Total used fuel at end of track for 25 generated topographies and measured topographies.

### 3 Road roughness modelling

Modelling of road profiles is an important area of transportation engineering as durability studies of vehicle components often require a customer or market specific load description. Desired properties of the models are robustness and simplicity, so that only a small number of parameters need to be used to describe and classify homogeneous parts of the road. It is also of interest to reconstruct road pro-

files based on roughness measurements, e.g. the so-called International Roughness Index (IRI), which is often available from road administration databases.

Stationary Gaussian loads have been extensively studied in the literature and used as models for road roughness. Early applications of bivariate Gaussian processes to model road surface roughness can be found in (Dodds & Robson, 1973). Direct Gaussian models are convenient since linear filter responses are Gaussian processes as well. Although models based on Gaussian distributions are standard in the field, see, for example, (Sun et al., 2001; Múčka, 2004) for some recent studies, most experts of vehicle engineering agree that road surfaces are not, in fact, accurately represented by a Gaussian distribution, see (Dodds & Robson, 1973). One reason for this is that the actual roads contain short sections with above-average irregularity. As shown in (Bogsjö, 2007*b*), such irregularities cause most of the vehicle fatigue damage. Therefore, several extensions of the Gaussian model has been proposed.

In (Charles, 1993), a non-stationary model is proposed that is constructed as a sequence of independent Gaussian processes of varying variances but with the same standardized spectrum. This approach was further developed in (Bruscella et al., 1999; Rouillard, 2004, 2009). The variability of variances was modelled by a discrete distribution taking a few values. In (Rouillard, 2004) random lengths of constant variance sections were also considered. In those papers the problem of connecting the segments with constant variances into one signal was not addressed and thus the response was modelled as a sequence of stationary Gaussian processes, i.e. by a process of the same type as the model of road surface. Another approach has been proposed in (Bogsjö, 2007*a*) where a bivariate road model was constructed based on a Gaussian process with added random irregularities.

In (Bogsjö et al., 2012) a new class of random processes, namely Laplace processes, has been proposed for modelling road profiles. Simply speaking it is Gaussian processes where the variance is randomly changing. In the current paper we present Laplace modelling based on (Bogsjö et al., 2012; Johannesson & Rychlik, 2014) and its extensions and applications presented in (Johannesson & Rychlik, 2013; Kvanström et al., 2013; Johannesson et al., 2015*a*; Kozubowski et al., 2013).

In the case when only IRI data are available, a simple enough model is required in order to be able to estimate the model parameters. Therefore, we will use the non-stationary Laplace model presented in (Bogsjö et al., 2012; Johannesson & Rychlik, 2014), together with the standardized spectrum according to (ISO 8608, 1995), which gives a Laplace model with only two parameters to estimate, where the first parameter describes the mean roughness, while the second parameter describes the variability of the variance which is gamma distributed. In this Laplace model the variance is constant for short segments of fixed length, typically one or some hundred metres. By using IRI data from the Finnish road network, we will demonstrate how to efficiently estimate the Laplace parameters, and evaluate their dependency on the type of road. Further, we will employ a simple but accurate approximation of the fatigue damage due to Laplace roads. Extensions of the Laplace model to parallel tracks and to multi-dimensional loads are also presented.

### 3.1 Road spectra and roughness coefficient

For stationary loads, power spectra are often used to describe the frequency content of a signal. The vertical road variability consists of the slowly changing landscape (topography), the road surface unevenness (road roughness), and the high variability components (road texture). For durability applications, the road roughness is the relevant part of the spectrum. Often one assumes that the energy for frequencies  $< 0.01 \text{ m}^{-1}$  (wavelengths above 100 metres) represents landscape variability, which does not affect the vehicle dynamics and hence can be removed from the spectrum. Similarly high frequencies  $> 10 \text{ m}^{-1}$  (wavelengths below 10 cm) are filtered out by the tire and thus are not included in the spectrum.

Following the ISO 8608 standard (ISO 8608, 1995), let us introduce the limits on the spectrum band of interest, viz.

$$\Omega_L = 2\pi/90 \text{ rad/m}, \quad \Omega_R = 2\pi/0.35 \text{ rad/m}. \quad (12)$$

Further, the ISO standard uses a two parameter spectrum to describe the road profile  $Z(x)$

$$S(\Omega) = C \left( \frac{\Omega}{\Omega_0} \right)^{-w}, \quad \Omega_L \leq \Omega \leq \Omega_R, \quad \text{and zero otherwise}, \quad (13)$$

where  $\Omega$  is the spatial angular frequency, and  $\Omega_0 = 1 \text{ rad/m}$ . The spectrum is parameterized by the degree of unevenness  $C$ , here called the roughness coefficient, and the waviness  $w$ . The ISO spectrum is often used for quite short road sections (in the order of 100 metres). For road classification the ISO standard uses a fixed waviness  $w = 2$ . This simplified ISO spectrum has only one parameter, the roughness coefficient  $C$ . The ISO standard and classification of roads have been discussed by many authors, e.g. recently in (González et al., 2008; Ngwangwa et al., 2010). The choice of the ISO spectra is motivated by its simplicity, as it depends on only one parameter that can be related to IRI, as will be explained below.

The simplicity of the ISO spectrum makes it attractive to use in vehicle development. However, often the spectrum parameterized as in ISO 8608 does not provide an accurate description of real road spectra, and therefore many different parameterizations have been proposed, see e.g. (Andrén, 2006) where several spectral densities  $S(\Omega)$  for modelling road profiles were compared. Further, in a study of roads in the USA, see (Kropáč & Múčka, 2008), estimated waviness values between 1 and 4 were found, with an average of  $w = 2.5$ . A typical waviness value of about 2.5 has also been reported by others, see e.g. (Andrén, 2006) for a study of Swedish roads and (Braun & Hellenbroich, 1991) for German roads. Therefore, two values of waviness will be used in this work, namely  $w = 2$  and  $w = 2.5$ .

We will also use an alternative parametrization of the ISO spectrum by introducing the normalized ISO spectrum

$$\tilde{S}(\Omega) = C_0(\Omega/\Omega_0)^{-w}, \quad C_0^{-1} = (\Omega_L^{1-w} - \Omega_R^{1-w}) / (w - 1) \quad (14)$$

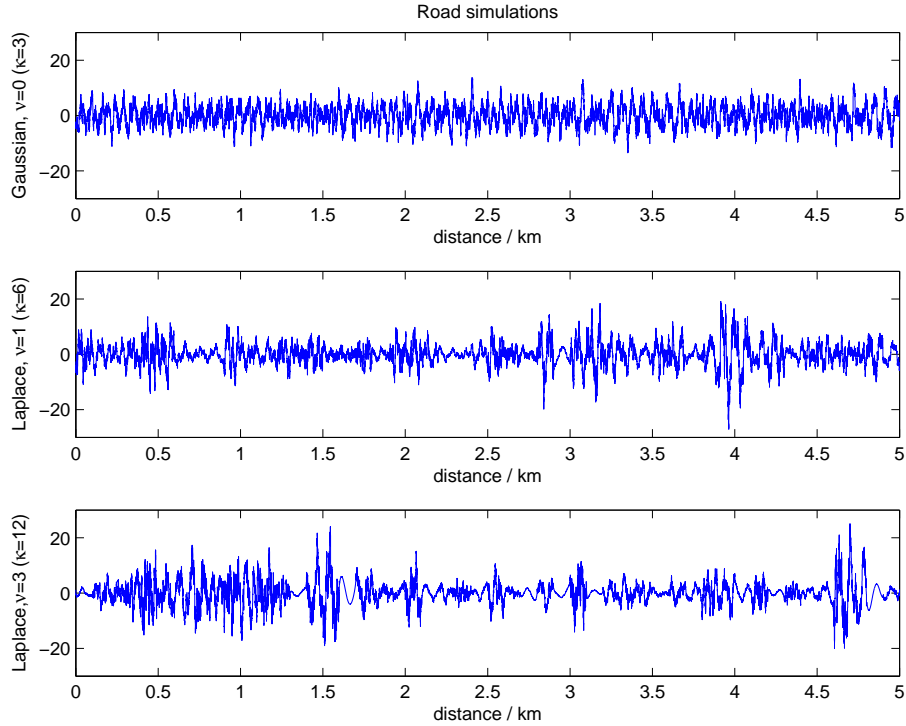


Figure 7: Simulations of road profiles; Laplace processes with different kurtosis,  $\kappa = 3, 6, 12$ ;  $\kappa = 3(\nu + 1)$ . (Note that Laplace with  $\kappa = 3$  gives the stationary Gaussian process).

such that  $\int \tilde{S}(\Omega) d\Omega = 1$ . Here  $C_0 = 0.0694 \text{ m}^3/\text{rad}$  if waviness  $w = 2$ , and  $C_0 = 0.0273 \text{ m}^3/\text{rad}$  if  $w = 2.5$ . Then  $\sigma^2 = C/C_0$  is the variance of the road profile  $Z(x)$ , and the ISO spectrum can be written as

$$S(\Omega) = \sigma^2 \tilde{S}(\Omega). \quad (15)$$

### 3.2 Laplace modelling of road profiles

Stationary Gaussian loads have been extensively studied in literature and applied as models for road roughness, see e.g. (Dodds & Robson, 1973) for an early application. However, the authors of that paper were aware that Gaussian processes cannot "exactly reproduce the profile of a real road". In (Charles, 1993) a non-stationary model was proposed, constructed as a sequence of independent Gaussian processes of varying standard deviations but the same standardized spectrum. Knowing durations and sizes of standard deviations the model is a non-stationary Gaussian process. Similar approaches were used in (Bruscella et al., 1999), and (Rouillard, 2004, 2009). The variability of the standard deviation was modelled by a discrete distribution taking a few number of values. In (Rouillard, 2009) random lengths of constant variance sections were also considered.

To summarize, the Gaussian model is frequently used for modelling road profiles. However, the Gaussian model is often only valid for short sections, say 100 m, whereas longer sections of roads, say 10 km, typically contain shorter sections with high irregularity, and the variability between sections is higher than can be explained by the stationary Gaussian model. This phenomenon can be captured by a Laplace process, which can be seen as a Gaussian process with randomly varying variance. Thus, the Gaussian process is a special case of the Laplace process. A Laplace process can be constructed by randomly varying the local variance, for segments of fixed length, according to a gamma distribution. Here we will employ the ISO road spectrum with waviness  $w = 2$ , see Eq. (13), and 100-metre segments, giving the Laplace-ISO model that can be described by only two parameters, namely its mean roughness,  $C$  and the Laplace shape parameter,  $\nu$  (or equivalently by its variance and kurtosis). The parameters can be estimated from a sequence of IRI-values, which is often available, and can then be used for reconstruction of road profiles. Simulated profiles for different Laplace shape parameters are shown in figure 7. More details on Laplace road models are found in (Bogsjö et al., 2012; Johannesson & Rychlik, 2014), including Matlab code for simulating Laplace-ISO road profiles. Further, in (Johannesson & Rychlik, 2014) the Laplace-ISO model was validated using eight road sections representing different types of roads as well as different geographical locations.

### 3.3 Stationary Gaussian model

A zero mean stationary Gaussian processes is completely defined by its power spectrum. There are several ways to generate Gaussian sample paths. The algorithm proposed in (Shinozuka, 1971) is often used in engineering. It is based on the spectral representation of a stationary process. Here we use an alternative way that expresses a Gaussian process as a moving average of white noise.

Roughly speaking a moving average process is a convolution of a kernel function  $g(x)$ , say, with an infinitesimal “white noise” process having variance equal to the spatial discretization step, say  $dx$ . Then a Gaussian process can be approximated by

$$Z(x) \approx \sum g(x - x_i) Z_i \sqrt{dx}, \quad (16)$$

where the  $Z_i$ 's are independent standard Gaussian random variables, while  $dx$  is the discretization step, here reciprocal of the sampling frequency (often  $dx = 5$  cm for road profiles). An appropriate choice of the length of the increment  $dx$  is related to the smoothness of the kernel. The kernel  $g(x)$  is conveniently defined by its Fourier transform, viz.

$$(\mathcal{F}g)(\Omega) = \sqrt{2\pi S(\Omega)}, \quad (17)$$

where  $\mathcal{F}$  stands for Fourier transform.

### 3.4 Stationary Laplace model

A stationary Laplace process can be constructed by extending the above Gaussian model, Eq. (16), by introducing gamma variables. The resulting Laplace Moving Average (LMA) process can be approximated by

$$Z(x) \approx \sum g(x - x_i) \sqrt{R_i} Z_i \sqrt{dx}, \quad (18)$$

where the  $R_i$ 's and the  $Z_i$ 's are independent gamma and standard Gaussian random variables, respectively. Note that  $\sqrt{R_i} Z_i$  has a generalized Laplace distribution, and it can be shown that  $Z(x)$  also has a generalized Laplace distribution. More details about the LMA model are found in (Åberg et al., 2009; Bogsjö et al., 2012; Kvanström et al., 2013). An application of the LMA model for cultivator loads will be shown in Section 4.2.

### 3.5 Local road roughness

Suppose that a 10 km long road is split into 100 metre segments, giving a sequence of estimates of the local roughness  $\hat{C}_j$ ,  $j = 1, \dots, 100$ , e.g. using Eq. (28) below. The observed variability of the estimates  $\hat{C}_j$  could be caused by statistical estimation errors and hence could be neglected. In such a case the road is stationary with spectral density (13) and mean roughness  $C$  estimated as the average of  $M$  roughness values

$$\hat{C} = \frac{1}{M} \sum_{j=1}^M \hat{C}_j. \quad (19)$$

Consequently the variance  $\sigma^2$  in Eq. (15) is estimated by

$$\hat{\sigma}^2 = \hat{C}/C_0, \quad (20)$$

The local variance can be written as  $\sigma_j^2 = r_j \cdot \sigma^2$  where the factor  $r_j$  is estimated as

$$r_j = \hat{C}_j/\hat{C}. \quad (21)$$

The variability of  $r_j$  is measured by means of its variance, denoted by  $\nu$  and estimated by

$$\hat{\nu} = \frac{1}{M-1} \sum_{j=1}^M (r_j - 1)^2. \quad (22)$$

Based on an extensive simulation study of 10 km long stationary Gaussian road profiles it was found that  $\hat{\nu}$  is only negligibly biased, with an estimated median bias of 0.017, and a 95% empirical quantile of 0.021. Hence, if  $\hat{\nu}$  is less than about 0.02, then we may assume that the variance  $\sigma^2$  is constant for the road profile and a stationary Gaussian model can be used, see Section 3.3.

However, quite often the variability of  $r_j$  is too large to be explained by solely statistical estimation errors. This type of variability calls for a special treatment.

For example, one could use different ISO spectra for each of the 100 metre road segments giving 100 parameters to describe the spectral properties of a 10 km long road. The result is a non-stationary Gaussian model, presented in Section 3.6. An alternative to this rather ad hoc procedure is to use a stochastic model for the variability of the factors  $r_j$ . Here we model  $r_j$  as gamma distributed random variables, having mean one and variance  $\nu$ , which results in the Laplace model presented in Section 3.7.

### 3.6 Non-stationary Gaussian model

The process consists of  $M$  segments of length  $L = L_p/M$  and we wish to define a process on  $[0, L_p]$ . Define the  $j$ :th non-stationary Gaussian process  $Z_j(x)$  process for all  $0 \leq x \leq L_p$ . Let again  $dx$  be the sampling step of the process and  $[s_{j-1}, s_j]$ ,  $s_j - s_{j-1} = L$ , the interval where the road profile model would have the local variance  $\sigma_j^2 = r_j \cdot \sigma^2$ , viz.  $s_0 = 0 < s_1 < \dots < s_M = L_p$ . Now define  $M$  processes  $Z_j(x)$  as follows

$$Z_j(x) \approx \sum_{s_{j-1} < x_i \leq s_j} g(x - x_i) \sqrt{r_j} Z_i \sqrt{dx}, \quad (23)$$

where the  $Z_i$ 's are independent standard Gaussian variables, and  $dx$  is the discretization step. Finally the road profile model  $Z(x)$  is given by

$$Z(x) = \sum_{j=1}^M Z_j(x). \quad (24)$$

### 3.7 Non-stationary Laplace model

The non-stationary Gaussian model for  $M$  road segments requires  $M$  parameters in order to model the variability in the variance, i.e. the varying local roughness. In order to reduce the number of parameters it is desirable to use a stochastic model for the sequence of  $r_j$ -values. A non-stationary Laplace process is obtained by modelling the  $r_j$ 's as gamma distributed random variables, and thus, only one parameter is needed to model the variability in the roughness, namely, the Laplace shape parameter  $\nu$ . By definition of the factors  $r_j$  in Eq. (21), the gamma factors have mean one and variance  $\nu$ . In order to completely define the Laplace model one also needs to specify the dependence structure of the sequence of factors  $r_j$ . The simplest Laplace model is obtained by assuming that the factors are independent, i.e. the roughness of the segments vary in an independent manner. Then, the non-stationary Laplace model can be described by one extra parameter  $\nu$ , compared to the stationary Gaussian model.

By replacing  $r_j$  in Eq. (23) by independent Gamma random variables  $R_j$ , we get

$$Z_j(x) \approx \sum_{s_{j-1} < x_i \leq s_j} g(x - x_i) \sqrt{R_j} Z_i \sqrt{dx}. \quad (25)$$

and the road profile  $Z(x)$  is given by

$$Z(x) = \sum_{j=1}^M Z_j(x). \quad (26)$$

Further, for a zero mean Gaussian random variable  $Z_j$ , the product  $\sqrt{R_j}Z_j$  has a generalized Laplace distribution, and thus the process  $Z(x)$ , defined in Eq. (26), has a generalized Laplace distribution, see (Kotz et al., 2001).

It seems reasonable to believe that the quality of the road surface varies slowly and hence the factors  $R_j$  defined in Eq. (21) are likely dependent between themselves. The degree of dependence is a function of the chosen length of the constant variance segments (here 100 metres). Therefore, an autoregressive model for the random variances  $R_j$  can be employed. In fact, the same gamma AR(1) model as presented for topography can be used for road roughness, see Eq. (37), thus introducing one extra parameter, the correlation  $a_r$ .

### 3.8 A simulation example

In Figure 8 two simulated road profiles are illustrated, both having ISO spectrum with waviness parameter  $w = 2$  and standard deviation  $C = 1 \cdot 10^{-6} \text{ m}^3$ . The factors  $R_j$  are gamma distributed with parameter  $\nu = 1$ , see Eq. (10). In the top plot the Laplace model has independent gamma distributed variances, while in the bottom plot the variances form an AR(1)-process with correlation  $a_r = 0.9$ . One can see that regions with larger/smaller variability are longer for correlated variances. Such a region may last for several kilometres. MATLAB code to simulate this model can be found in Appendix A.2.

### 3.9 International Roughness Index

When monitoring road quality, segments of measured longitudinal road profiles are often condensed into a sequence of IRI values, see (Gillespie et al., 1986). They are calculated using a quarter-car vehicle model, see Figure 9, whose response at speed 80 km/h is accumulated to yield a roughness index with units of slope (e.g. mm/m). More precisely, IRI is defined as the accumulated suspension motion divided by the distance travelled. The parameters of the quarter vehicle are defined by the so-called Golden Car with parameters given in Figure 9. Since its introduction in 1986, IRI has become the road roughness index most commonly used worldwide for evaluating and managing road systems. Thus, IRI parameters are often available from road databases maintained by road agencies and are typically reported for each 20 or 100 metres.

For a Gaussian road profile with ISO spectrum the expected IRI can be computed as

$$E[\text{IRI}] = 2.21 \cdot 10^3 \cdot \sqrt{C}, \quad E[\text{IRI}] = 1.91 \cdot 10^3 \cdot \sqrt{C} \quad (27)$$

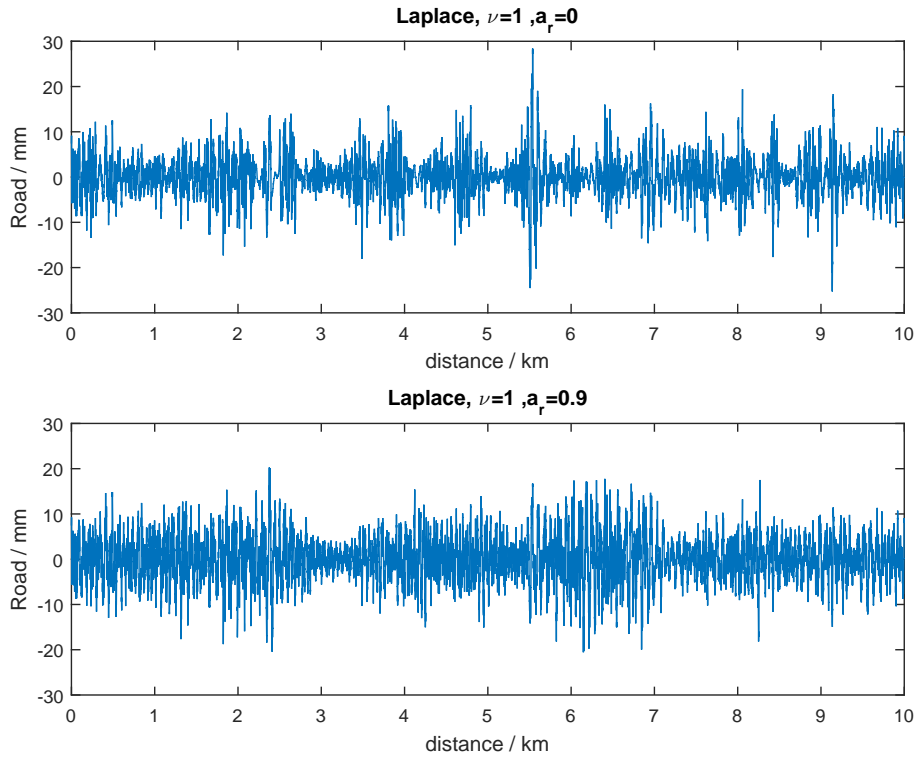


Figure 8: Comparison of 10 km simulated Laplace models having ISO spectrum, with waviness parameter  $w = 2$  and parameters  $C = 1 \cdot 10^{-6} \text{ m}^3$  and  $\nu = 1$ . The variance of the factors  $R_j$  is  $\nu = 1$ . Top graph has independent random factors ( $a_r = 0$ ) and the bottom graph has correlated AR(1) factors with  $a_r = 0.9$ .

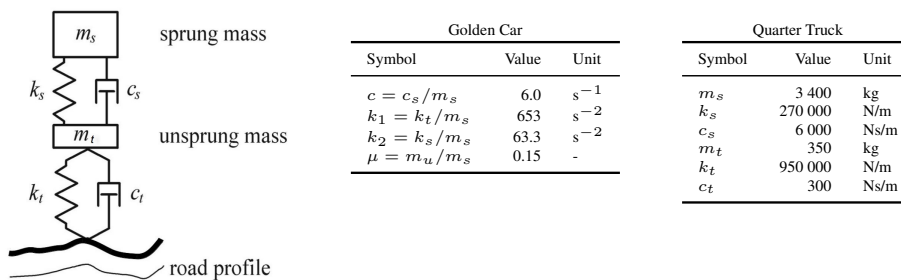


Figure 9: Quarter vehicle model.

Table 1: Road classes of Finnish roads.

Functional class	Number of sections
1 = main road	1 131
2 = main road 2nd class	577
3 = local road	1 479
4 = connecting road	2 204

for waviness  $w = 2, 2.5$ , respectively, where the roughness coefficient  $C$  has units  $\text{m}^3/\text{rad}$ . The theoretically derived relationship between IRI and  $C$  can be generalized to arbitrary waviness and speed, see (Sun et al., 2001), (Johannesson & Rychlik, 2014), and (Kropáč & Múčka, 2004, 2007).

For completeness, we give formulas to estimate the parameter  $C$  in the ISO spectrum (13) if the IRI value is known, viz.

$$\hat{C}_j = 10^{-6} \cdot \left( \frac{\hat{I}_j}{2.21} \right)^2, \quad \hat{C}_j = 10^{-6} \cdot \left( \frac{\hat{I}_j}{1.91} \right)^2 \quad (28)$$

for  $w = 2, 2.5$ , respectively, where  $\hat{I}_j$  is an estimate of IRI in unit  $\text{mm}/\text{m}$  and  $\hat{C}_j$  has unit  $\text{m}^3/\text{rad}$ .

### 3.10 Laplace modelling of roads in Finland

We here present results on Laplace modelling of Finnish roads, where we have IRI values for 100 metre road segments. The data have been obtained from the Finnish Transport Agency. In total there are 5391 road sections longer than 5 km. Most of the road sections are between 5 and 10 kilometres. The goal here is to describe and classify roads according to the Laplace parameters and relate these to the functional class, see Table 1.

For each longer section (at least 5 km) of the roads, Laplace models have been estimated based on the sequence of IRI-values. First the  $C$ -values for 100 metre segment are estimated from IRI-values by using Eq. (28) with  $w = 2$ . In the second step the Laplace parameters are estimated, according to

$$\hat{C} = \frac{1}{M} \sum_{j=1}^M \hat{C}_j, \quad \hat{\nu} = \frac{\frac{1}{M-1} \sum_{j=1}^M (\hat{C}_j - \hat{C})^2}{\hat{C}^2}. \quad (29)$$

i.e. the roughness coefficient  $\hat{C}$  is the mean roughness, and the Laplace shape parameter  $\hat{\nu}$  is the coefficient of variation squared, see (Johannesson & Rychlik, 2014) for details. Once the Laplace parameters have been estimated from IRI-values, it is possible to stochastically reconstruct a road profile, see Figure 7 for examples. However, here we will investigate the variability of the Laplace parameters, and thus Box plots of the estimated parameters are presented in Figure 10 for different road classes.

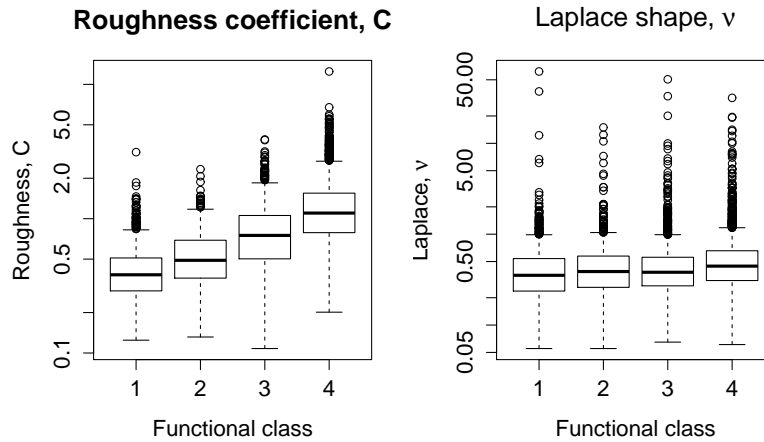


Figure 10: Estimated parameters  $C$  and  $\nu$  of Laplace models for roads in Finland.

Table 2: Distribution of Laplace parameters for different functional classes.

Functional class	Roughness, $C$ [ $\text{m} \cdot \text{mm}^2$ ]		Laplace, $\nu$	
	median	std-log	median	std-log
1	0.39	0.43	0.37	0.65
2	0.50	0.47	0.41	0.71
3	0.73	0.54	0.41	0.66
4	1.12	0.54	0.47	0.67

In Figure 10 we can observe that there is high variability in the estimates. However, it can be clearly seen that the roughness  $C$  increases with functional class, which is what can be expected. However, for the Laplace parameter  $\nu$  there are no clear tendencies, but rather that it seems to be independent of the functional class. We have investigated the distribution of the Laplace parameters within a certain functional class by making normal probability plots. The conclusion was that the log-normal distribution fits reasonably well. Therefore, it seems adequate to characterize the distribution of the logarithmic Laplace parameters by their mean and standard deviation, see Table 2, where the median of the parameter is presented, instead of the logarithmic mean, calculated as:  $\text{median}(C) = \exp(\ln C)$ .

As it was concluded before, the median roughness increases with the functional class, while the median of the Laplace shape parameter does not seem to depend on the functional class and the median Laplace parameter is about 0.4 (i.e. slightly non-Gaussian). The standard deviations in log-scale can be interpreted as the relative scatter, and it does not seem to depend on the functional class. For the roughness it is about 0.5 and for the Laplace parameter it is about 0.7. The conclusion is that, for the Finnish roads, only the median roughness depends on the functional class, while the median Laplace parameter and the relative scatters

do not depend on the functional class.

We have demonstrated that for a certain functional class, the Laplace parameters may be characterized by their medians and relative scatters, where only the median roughness varies between different classes for the Finnish roads. This characterization of road types can be useful for reconstruction of roughness parameters for roads in regions where there are no roughness data available. In such a case the roughness parameters could be reconstructed based on, for example, road type (e.g. functional class) and the general standard of the region (e.g. obtained from socio-economic data).

### 3.11 Fatigue damage due to Laplace road profiles

We will here define a fatigue damage index that is assessed by studying the response of a quarter-vehicle model travelling at a constant speed on road profiles, see Figure 9. To be more precise, the response considered is the force acting on the sprung mass. Such a simplification of a physical vehicle cannot be expected to predict loads exactly, but it will highlight the most important road characteristics as far as fatigue damage accumulation is concerned. The parameters in the model are set to mimic heavy vehicle dynamics, following (Bogsjö, 2007b). Thus, the values of the parameters differ somewhat from the ones defining the Golden car. The force response of the quarter-vehicle can be computed through linear filtering of the road profile. The purpose of this work is to propose models for road profiles defined by means of a few parameters that could be used to compute the vehicle response, and hence the most important criterion for a good model of a measured road profile is that the rainflow damage of the response is well represented. Thus, the fatigue damage index is defined by using rainflow cycle counting of the response in combination with the Palmgren-Miner rule, see (Palmgren, 1924; Miner, 1945) for details.

A practically important theoretical result on the expected damage for the Laplace-ISO model is presented in (Johannesson & Rychlik, 2014). The expected damage index, with damage exponent  $k$ , for a Laplace-ISO road with waviness  $w = 2$  and parameters  $(C, \nu)$  can be approximated by an explicit algebraic expression

$$E[D_s(k, C, \nu)] \approx 0.07093e^{13.92k} \left(\frac{C}{C_0}\right)^{k/2} \left(\frac{s}{s_0}\right)^{k/2-1} \nu^{k/2} \frac{\Gamma(k/2 + 1/\nu)}{\Gamma(1/\nu)}, \quad (30)$$

where the reference values are  $C_0 = 1/14.4 \text{ m}^3$  and  $s_0 = 10 \text{ m/s}$ . The first factor depends on the parameters of the quarter-vehicle response, and the coefficients have been estimated from a long simulation of a Gaussian road. The coefficients 0.07093 and 13.92 will be different for another filter. The second factor is a correction for the average roughness  $C$ . The third factor is a correction for the vehicle speed  $s$ . The last factor is a correction for the Laplace model, depending only on the Laplace shape parameter  $\nu$ .

As an example, we have computed the expected damage under Gaussian and

Laplace model assumptions for the Finnish roads, see Figure 11. Damage exponent  $k = 5$  and vehicle speed 80 km/h were used in the damage calculations. We can see that the Laplace model predicts higher damages compared to the Gaussian model, which is due to the correction factor depending on the Laplace shape parameter  $\nu$ .

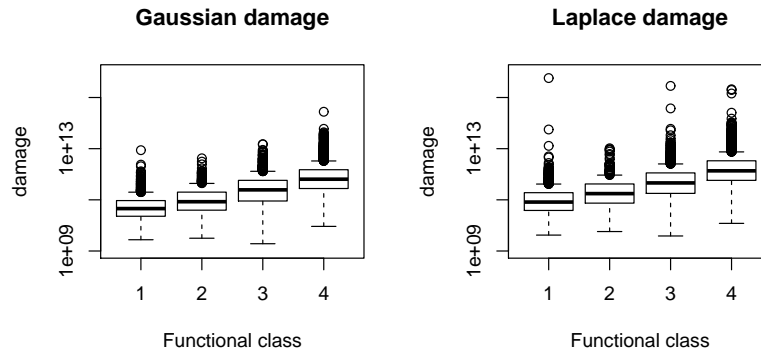


Figure 11: Theoretically computed expected damage for Gaussian and Laplace models.

## 4 Multi-dimensional Laplace models

Here we give extensions of the Laplace models to situations of multiple correlated signals, e.g. road profiles along two parallel tracks and multi-dimensional loads. First a non-stationary Laplace model of road profiles along two parallel paths taken by left and right wheels of a vehicle are presented, following (Kozubowski et al., 2013; Johannesson et al., 2015a). Then a stationary multi-dimensional Laplace model is presented, as described in (Kvanström et al., 2013), with an example on cultivator loads.

### 4.1 Two-track Laplace models

Considering just a single path along the road can be an oversimplification, as any four-wheeled vehicle is subjected to excitations due to road roughness in the left as well as the right wheel paths. Thus, accounting for both the paths should be an important aspect of vehicle fatigue assessment. Hence, it is natural to search for an adequate and effective bivariate stochastic model corresponding to parallel road tracks. The spectral representation of a 2-track Laplace process is the same as for a standard 2-track Gaussian one, namely the left and right tracks are described by the spectra  $S_L(\Omega)$ ,  $S_R(\Omega)$  and the cross-spectra  $S_{LR}(\Omega) = S_{RL}(\Omega)$ , see e.g. (Dodds & Robson, 1973; Bogsjö, 2007a). The work is an extension to parallel track of the single track models presented in (Johannesson & Rychlik, 2014; Bogsjö et al., 2012). It can be interpreted as a Gaussian vector valued process where the local variance is randomly varying according to a gamma distribution. More precisely,

left and right road profiles,  $Z_L(x)$  and  $Z_R(x)$ , respectively, are assumed to be Gaussian with variances that vary between short road segments. The value of the variance is random between the short road segments and varies according to a gamma distribution, introducing the Laplace shape parameter  $\nu$ .

In our example the ISO spectrum is employed for both left and right tracks

$$S_L(\Omega) = S_R(\Omega) = C \left( \frac{\Omega}{\Omega_0} \right)^{-w}, \quad \Omega_1 \leq \Omega \leq \Omega_2 \text{ rad/m}, \quad \Omega_0 = 1 \text{ rad/m}, \quad (31)$$

and the dependence between left and right tracks is modelled by an exponentially decreasing normalized cross-spectrum

$$K_{LR}(\Omega) = \frac{|S_{LR}(\Omega)|}{\sqrt{S_L(\Omega)S_R(\Omega)}} = \exp(-b|\Omega|). \quad (32)$$

It was demonstrated in (Bogsjö, 2008) that this simple normalized cross-spectrum, with only one parameter, describes the correlation between the tracks in many measured signals rather well. Note that the (squared) coherence spectrum is  $|K_{LR}(\Omega)|^2$ .

Based on the spectral representation there are methods to simulate Gaussian and Laplace roads, see (Kozubowski et al., 2013; Johannesson et al., 2015a). The algorithm and Matlab code to simulate the signal is presented in Appendix A.3. As an illustration three 2-track Laplace profiles with  $\nu = 0, 1, 3$  have been simulated, see Figure 12 showing the distance between 2 and 2.5 km. Note that  $\nu = 0$  represents the Gaussian case, compare Figure 7. It can be observed that the long wavelengths are highly correlated while the short wave lengths (high frequency oscillations) are almost uncorrelated. This is a result of the exponentially decreasing normalized cross-spectrum. Further examples on e.g. measured road profiles and fatigue damage are presented in (Johannesson et al., 2015a).

## 4.2 Multi-dimensional Laplace moving average models

In the previous section we have used a Laplace model for the road surface roughness along two parallel tracks. The method assumes that the two signal have the same statistical properties, i.e. the same power spectral densities and variances  $\nu$  of the factors  $R_k$ . Actually the same factors  $R_k$  are used in the signals which gives the effect that the high roughness parts occur frequently at the same positions on the tracks. The dependence between the two signals is defined by the cross-spectrum. However there are cases when the loads, constituted of transients, are correlated but not equally distributed. For such loads new type of model is needed.

Independent Laplace loads can be simulated using independent Gaussian noises and gamma factors, see Eq. (18). However it can lead to oversimplifications for loads where the transients tend to occur simultaneously in the loads. (Obviously the independent Laplace loads are lacking the property.) In (Kvanström et al., 2013) a general multi-dimensional Laplace model was given to handle correlated

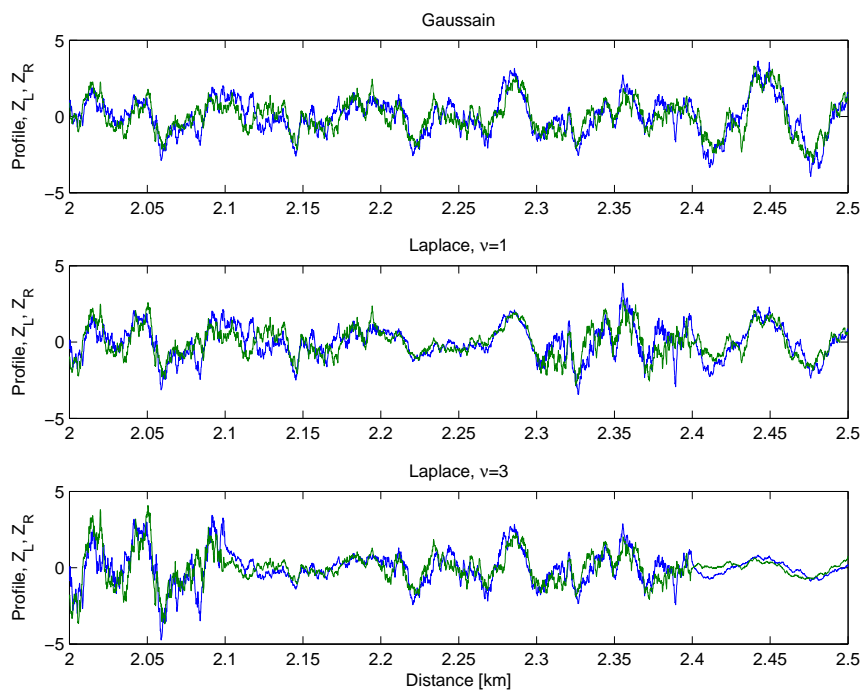


Figure 12: Simulation of three different 2-track Laplace roads.

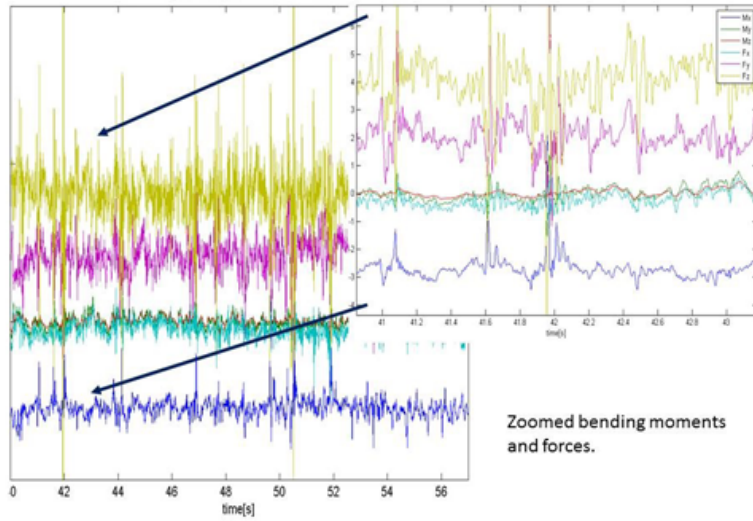


Figure 13: Measured forces and bending moments at one location of cultivator frame

and identically distributed Laplace loads. The mathematical details are quite complicated however the resulting algorithms to simulate multi-dimensional Laplace loads is simple. It is presented in Appendix A.3. The limitation of the method is that the loads have cross-spectra defined by the correlations between instantaneous values of the loads and the PSD of signals which may differ from the actual ones, see (Kvanström et al., 2013) for details. A general Laplace model for not identically distributed multi-dimensional loads having any cross spectra is not known yet.

In this section, we will apply the multi-dimensional Laplace model, to describe variability of forces and bending moments, measured at some point of a stiff mechanical structure. The method was used in (Kvanström et al., 2013) to assess the durability of welds in a stiff frame of a cultivator. For a stiff frame, stresses are linear combinations of environmental loads. In Figure 4.2, six loads, measured on one tine, are presented. In the figure one can see that transients appearing in different forces and bending moments are often close in time. Since stress is a linear combination of the loads this may result in very large stresses which may greatly amplify the fatigue damage accumulation rate in a weld.

In the present example we are modelling responses (forces and bending moments) which are filtered external loads and may have different PSDs as well kurtosis. This implies that the random factors  $R$ , used in the definition of Laplace signal, may have different gamma distributions, i.e. variances  $\nu$ .

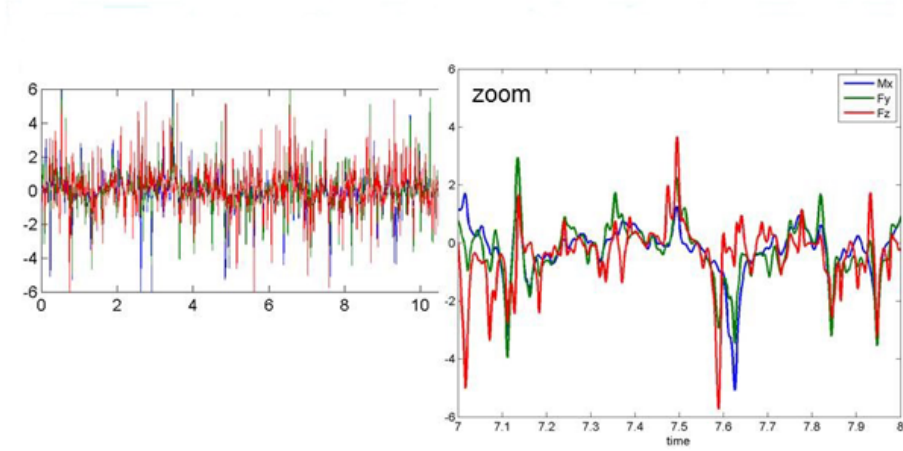


Figure 14: *Left*: Simulation of the Laplace model for standardized loads ( $F_y, F_z, M_x$ ), having mean zero and variance one.

### 4.3 Loads on cultivator frame

The multivalued Laplace method do not make any limitation for the load components spectra. However, it is desirable to use spectra dependent on few parameters which can vary between different environments, e.g. sandy or clay soil when the cultivator is working. For modelling cultivator loads, the following PSD proves to be useful

$$S(\omega) = 0.5\sigma^2 a_c \exp(-a_c|\omega|). \quad (33)$$

For the particular case of exponential spectrum this leads to

$$g(t) = \frac{2\sigma/\sqrt{\pi}}{1 + 4(t/a_c)^2}. \quad (34)$$

The parameter  $a_c$  governs steepness of transients while  $\sigma$  their average energy.

In Figure 4.2 one can see that forces  $F_y, F_z$  and the bending moment  $M_z$  are dominating signals and, for simplicity of presentation only, those three signal will be used in this example. Further, we will normalize the signal so that these have mean zero and variance ( $\sigma^2$ ) one. The estimated parameters  $a_c, (a_{F_y}, a_{F_z}, a_{M_x})$  equal to (0.012, 0.009, 0.015) while the signals kurtosis The kurtosis of the loads are ( $\kappa_{F_y}, \kappa_{F_z}, \kappa_{M_x}$ ) equal to (11.4, 9.4, 20.1). For the parameters the variances  $\nu$  of the factors  $R_k$  can be evaluated using the following formula

$$\nu = 0.42(\kappa - 3) a_c, \quad (35)$$

see (Rychlik, 2013) for more detailed presentation. Note that as  $\kappa$  tends to 3 the Laplace model approaches the Gaussian model. The parameters ( $\nu_{F_y}, \nu_{F_z}, \nu_{M_x}$ ) are equal to (0.042, 0.024, 0.108), respectively. The loads are correlated; correlation between  $M_x$  and  $F_y$  is 0.9;  $M_x$  and  $F_z$  is 0.3; correlation  $F_y$  and  $F_z$  is 0.5.

Using the program given in Appendix A.4 the standardized Laplace loads  $F_y$ ,  $F_z$ ,  $M_z$  were simulated and the results are presented in Figure 14. One can see that the transients observed in the loads are present in the Laplace model. Those are missing in commonly used Gaussian model. Finally we give the marginal fatigue damage indexes estimated using the Laplace models and the Gaussian models and compare it with the observed indexes, i.e. computed using the observed loads. The results are presented in Table 3. One can see that the observed damages agrees well with estimates based on Laplace models while the Gaussian model underestimate the damages due to lack of transients.

DAMAGE INDEX			
Data	$F_y$	$F_z$	$M_x$
observed	369	518	56
Laplace model	335	497	56
Gaussian model	151	245	19

Table 3: Observed damage index for loads  $F_y$ ,  $F_z$ ,  $M_x$  compared with the expected damage indexes for Laplacian and Gaussian models.

## 5 Conclusions

### Topography modelling

We discuss the classical Gaussian autoregressive models and an extension that accounts for non-Gaussian distribution of the records, thus providing a more flexible representation of observed topography data. The extended model has two components: the first one is given by a classical Gaussian AR(1) time series, while the second one represents the randomly varying variance given by an autoregressive gamma process. The dependence in the model is governed by two autoregressive parameters:  $a$  for the Gaussian AR(1) part and  $a_r$  for the autoregressive gamma part. The distributional parameters; location, scale and shape are obtained by fitting sample mean, variance and kurtosis to their sample equivalents. The models have been successfully used to investigate fuel consumption of an articulated hauler, where the generated topographies produce, with high accuracy, similar fuel consumptions as the ones induced by the real topography records. Understanding the topography environment is a key for evaluation of customer fuel consumption. The proposed simple AR(1) models give possibility to efficiently log sufficient information on topography, and can be used for vehicle on-board logging of topography to investigate and understand customer behaviour.

## Roughness modelling

Laplace models have proved to be useful for modelling measured road profiles with application to fatigue, see the validation studies in (Bogsjö et al., 2012; Johannesson & Rychlik, 2014; Johannesson et al., 2015a). The conclusions of the validation studies, with road sections represent different types of roads as well as different geographical location, can be summarized as follows

1. We have demonstrated that the Laplace model having observed spectrum reproduces the damage indices very well.
2. We investigated whether the simpler ISO spectrum could be used instead, and a useful Laplace-ISO model could be found for the studied roads.
3. We found that the presented approach to estimate Laplace-ISO models from IRI sequences is useful for reconstruction of road profiles when profile measurements are not available.

The third point has been of special industrial interest, since often measured road profiles are not available, but only condensed roughness data are available from road agencies in the form of IRI values or roughness coefficients. Then a simple statistical model for the road profile is needed in order to be able to estimate the model parameters. However, the model should still be useful for durability applications. For this purpose, the Gaussian model has been found to be too simple, see e.g. (Bogsjö, 2007b), since it cannot correctly capture the variability of the roughness. For our setup we have found that the Laplace-ISO model, i.e. a non-stationary Laplace model, (Bogsjö et al., 2012), with ISO spectrum (ISO 8608, 1995), is simple enough but still useful for durability evaluations, see (Johannesson & Rychlik, 2014). It can be interpreted as a Gaussian process where the local variance is randomly varying according to a gamma distribution. The length of constant variance segments is predefined, and for road profiles typically one or some hundred metres. Especially there are three good properties of the Laplace-ISO road model

- a small number of parameters are needed to define the model, namely the roughness coefficient,  $C$ , the Laplace shape parameter,  $\nu$ , and the length of constant variance road segment,  $L$ ,
- the parameters  $C$  and  $\nu$  can be estimated from the sequence of IRI, which is often available, and can then be used for reconstruction of road profiles, and
- the expected damage of a response of a vehicle, modelled by a linear filter, having Laplace-ISO road as an input, can be accurately approximated by an explicit formula depending only on the Laplace parameters, the damage exponent and the speed.

The last property is particularly convenient for sensitivity studies since lengthy simulations can be avoided. It can also be used for estimation of Laplace parameters and for classification purposes. The usefulness of the Laplace-ISO model was demonstrated for Finnish roads, where it was found that only the mean roughness varies between different road types, while no effect on the Laplace shape parameter was found. Lastly, it was demonstrated that the Laplace-ISO model can be extended to two-track road profiles.

### **Multivariate track models**

Two types of multivariate Laplace model have been presented. The first deals with road profiles along parallel tracks and assumes that the distribution of individual track are the same and follow the Laplace-ISO model. The dependence has been introduced by a cross-spectrum. The explicit simulation algorithm for the model is presented.

The second multivariate model allows for different distributions for individual components. It aims at modelling multivariate responses that have transients arising from a common source. The model has been successfully applied to model forces and moments on a cultivator frame and is validated by comparison of damage indexes. The results show that the Laplace model delivers much better accuracy in assessing damage when compared to the Gaussian model. An algorithm for simulation of this model is also given.

### **Acknowledgments**

The first author acknowledge partial support by the Swedish Energy Agency. The second author was partially supported by the Swedish Research Council Grant Dnr: 2013-5180. The third author acknowledge partial support by Knut and Alice Wallenberg stiftelse. Further, we are thankful to Volvo, Scania and Väderstad-Verken for supplying us with data.

### **References**

- Åberg, S., Podgórski, K. and Rychlik, I. (2009), ‘Fatigue damage assessment for a spectral model of non-Gaussian random loads’, *Probabilistic Engineering Mechanics*, Vol. 24, pp. 608 – 617.
- Andrén, P. (2006), ‘Power spectral density approximations of longitudinal road profiles’, *International Journal of Vehicle Design*, Vol. 40, pp. 2–14.
- Bogsjö, K. (2007a), ‘Evaluation of stochastic models of parallel road tracks’, *Probabilistic Engineering Mechanics*, Vol. 22, pp. 362–370.
- Bogsjö, K. (2007b), Road Profile Statistics Relevant for Vehicle Fatigue, PhD thesis, Mathematical Statistics, Lund University.

- Bogsjö, K. (2008), 'Coherence of road roughness in left and right wheel-path', *Vehicle System Dynamics: International Journal of Vehicle Mechanics and Mobility*, Vol. 46, pp. 599–609.
- Bogsjö, K., Podgorski, K. and Rychlik, I. (2012), 'Models for road surface roughness', *Vehicle System Dynamics*, Vol. 50, pp. 725–747.
- Braun, H. and Hellenbroich, T. (1991), Messergebnisse von Strassenunebenheiten, VDI-Berichte Nr. 877, pp. 47–80, VDI-Verlag, Dusseldorf.
- Brodtkorb, P. A., Johannesson, P., Lindgren, G., Rychlik, I., Rydén, J. and Sjö, E. (2000), WAFO – a Matlab toolbox for analysis of random waves and loads, in 'Proceedings of the 10th International Offshore and Polar Engineering conference, Seattle', Vol. III, pp. 343–350.
- Bruscella, B., Rouillard, V. and Sek, M. (1999), 'Analysis of road surfaces profiles', *Journal of Transportation Engineering*, Vol. 125, pp. 55–59.
- Charles, D. (1993), 'Derivation of environment descriptions and test severities from measured road transportation data', *Journal of the IES*, Vol. 36, pp. 37–42.
- Dodds, C. J. and Robson, J. D. (1973), 'The description of road surface roughness', *Journal of Sound and Vibration*, Vol. 31, pp. 175–183.
- Edlund, S. and Fryk, P.-O. (2004), 'The right truck for the job with global truck applications', SAE Technical Paper 2004-01-2645.
- Gillespie, T. D., Sayers, M. W. and Queiroz, C. A. V. (1986), The international road roughness experiment: Establishing correlation and calibration standard for measurement, Technical Report No. 45, The World Bank.
- González, A., O'brie, E. J., Li, Y.-Y. and Cashell, K. (2008), 'The use of vehicle acceleration measurements to estimate road roughness', *Vehicle System Dynamics*, Vol. 46, pp. 483–499.
- ISO 8608 (1995), 'Mechanical vibration - road surface profiles - reporting of measured data, ISO 8608:1995(E)', International Organization for Standardization, ISO.
- Johannesson, P. and Rychlik, I. (2013), 'Laplace processes for describing road profiles', *Procedia Engineering*, Vol. 66, pp. 464 – 473. Fatigue Design 2013, International Conference Proceedings.
- Johannesson, P. and Rychlik, I. (2014), 'Modelling of road profiles using roughness indicators', *Int. J. Vehicle Design*, Vol. 66, pp. 317–346.
- Johannesson, P., Podgórski, K. and Rychlik, I. (2015a), 'Modelling roughness of road profiles on parallel tracks using roughness indicators', Accepted for publication in *Int. J. Vehicle Design*.

- Johannesson, P., Podgórski, K., Rychlik, I. and Shariati, N. (2015b), ‘AR(1) time series with autoregressive gamma variance for road topography modeling’, Accepted for publication in *Probabilistic Engineering Mechanics*.
- Kotz, S., Kozubowski, T. J. and Podgórski, K. (2001), *The Laplace Distribution and Generalizations: A Revisit with Applications to Communications, Economics, Engineering and Finance*, Birkhäuser, Boston.
- Kozubowski, T. J. and Podgórski, K. (2008), ‘Skew Laplace distributions ii. Divisibility properties and extensions to stochastic processes’, *The Mathematical Scientist*, Vol. 33, pp. 35–48.
- Kozubowski, T. J., Podgórski, K. and Rychlik, I. (2013), ‘Multivariate generalized Laplace distribution and related random fields’, *Journal of Multivariate Analysis*, Vol. 113, pp. 59–72.
- Kropáč, O. and Múčka, P. (2004), ‘Non-standard longitudinal profiles of roads and indicators for their characterization’, *International Journal of Vehicle Design*, Vol. 36, pp. 149–172.
- Kropáč, O. and Múčka, P. (2007), ‘Indicators of longitudinal road unevenness and their mutual relationships’, *Road Materials and Pavement Design*, Vol. 8, pp. 523–549.
- Kropáč, O. and Múčka, P. (2008), ‘Indicators of longitudinal unevenness of roads in the USA’, *International Journal of Vehicle Design*, Vol. 48, pp. 393–415.
- Kvanström, M., Podgórski, K. and Rychlik, I. (2013), ‘Laplace moving average model for multi-axial responses in fatigue analysis of a cultivator’, *Probabilistic Engineering Mechanics*, Vol. 34, pp. 12–25.
- Miner, M. A. (1945), ‘Cumulative damage in fatigue’, *Journal of Applied Mechanics*, Vol. 12, pp. A159–A164.
- Múčka, P. (2004), ‘Road waviness and the dynamic tyre force’, *International Journal of Vehicle Design*, Vol. 36, pp. 216–232.
- Ngwangwa, H. M., Heyns, P. S., Labuschagne, F. J. J. and Kululanga, G. K. (2010), ‘Reconstruction of road defects and road roughness classification using vehicle responses with artificial neural networks simulation’, *Journal of Terramechanics*, Vol. 47, pp. 97–111.
- Palmgren, A. (1924), ‘Die Lebensdauer von Kugellagern’, *Zeitschrift des Vereins Deutscher Ingenieure*, Vol. 68, pp. 339–341. *In German*.
- Rouillard, V. (2004), ‘Using predicted ride quality to characterise pavement roughness’, *International Journal of Vehicle Design*, Vol. 36, pp. 116–131.

- Rouillard, V. (2009), ‘Decomposing pavement surface profiles into a Gaussian sequence’, *International Journal of Vehicle Systems Modelling and Testing*, Vol. 4, pp. 288–305.
- Rychlik, I. (2013), ‘Note on modelling of fatigue damage rates for non-Gaussian stresses’, *Fatigue & Fracture of Engineering Materials & Structures*, Vol. 36, pp. 750–759.
- Schwarzer, V., Ghorbani, R. and Rocheleau, R. (2010), Drive cycle generation for stochastic optimization of energy management controller for hybrid vehicles, in ‘Proceedings of the IEEE International Conference on Control Applications’, pp. 536–540.
- Shinozuka, M. (1971), ‘Simulation of multivariate and multidimensional random processes’, *The Journal of the Acoustical Society of America*, Vol. 49, pp. 357–368.
- Sim, C. H. (1971), ‘First-order autoregressive models for gamma and exponential processes’, *Journal of Applied Probability*, Vol. 27, pp. 325–332.
- Souffran, G., Miegerville, L. and Guerin, P. (2012), ‘Simulation of real-world vehicle missions using a stochastic Markov model for optimal powertrain sizing’, *IEEE Transactions on Vehicular Technology*, Vol. 61, pp. 3454–3465.
- Sun, L., Zhang, Z. and Ruth, J. (2001), ‘Modeling indirect statistics of surface roughness’, *Journal of Transportation Engineering*, Vol. 127, pp. 105–111.
- WAFO Group (2011a), ‘WAFO – a Matlab toolbox for analysis of random waves and loads, tutorial for WAFO 2.5’, Mathematical Statistics, Lund University.
- WAFO Group (2011b), ‘WAFO – a Matlab Toolbox for Analysis of Random Waves and Loads, Version 2.5, 07-Feb-2011’, Mathematical Statistics, Lund University.  
 Web: <http://www.maths.lth.se/matstat/wafo/> (Accessed 24 November 2015).

## Appendix

### A MATLAB code for model simulation

For readers convenience we present the MATLAB codes used to simulate the Gaussian and Laplace models for both road topography and road profile. In the code some functions from the WAFO toolbox (Brodtkorb et al., 2000; WAFO Group, 2011a) are used, which can be downloaded free of charge, (WAFO Group, 2011b). The statistical functions `rndnorm`, `rndgam`, `rndpois` and `rndexp`

are also available in the MATLAB statistics toolbox through `normrnd`, `gamrnd`, `poissrnd` and `exprnd`. Note that WAFO also contains functions to find rain-flow ranges used to estimate fatigue damage.

### A.1 Simulation of Laplace road topography model

We begin by explaining the models for simulation and then we present a MATLAB script to simulate the discussed model, resulting in stochastically generated topographies.

Recall that the classical Gaussian AR(1)-process  $X_k$  having mean zero and variance one, is defined by a recursion

$$X_k = a X_{k-1} + \sqrt{1 - a^2} e_k, \quad (36)$$

where  $e_k$  are independent zero mean variance one Gaussian variables (Gaussian white noise). Further, the parameter  $a$  is the one-step correlation. Defining a gamma distributed AR(1)-process is a more difficult problem which is discussed in (Johannesson et al., 2015a). The gamma AR(1)-process for  $R_k$  can be defined by a recursion similar to the Gaussian AR(1)-process, viz.

$$R_k = a_r K(R_{k-1}) \cdot R_{k-1} + (1 - a_r) \epsilon_k, \quad (37)$$

where  $a_r \in (0, 1)$  is an autoregressive coefficient,  $\epsilon_k$ 's are mutually independent gamma distributed variables – random innovations – with mean one and variance equal to the parameter  $\nu$ , independent also from  $K_k = K(R_{k-1})$  and  $R_{k-1}$ . Here the random factor  $K(r)$  is given by

$$K(r) = \frac{1}{m(r)} \sum_{i=0}^{N(r)} E_i, \quad (38)$$

where  $E_i$ 's are independent random variables,  $E_0 = 0$  while, for  $i > 0$ ,  $E_i$ 's are exponentially distributed and independent of the Poisson random variable  $N(r)$  having mean  $m(r)$  equal to

$$m(r) = \frac{a_r}{1 - a_r} \frac{r}{\nu}. \quad (39)$$

It can be shown that this model has exponentially decaying autocorrelation  $a_r^k$ ,  $k = 0, 1, \dots$ , see (Sim, 1971), where the gamma autoregressive model has been introduced, or (Kozubowski & Podgórski, 2008), where a historical overview and further properties of this model are presented.

```
>> N=1320;
>> sy=3.71; nu=1.11;
>> a=0.734; a_r=0.84;
>> rAR=zeros(N,1); xAR=zeros(N,1);
>> riid=nu*rndgam(1/nu,1,N,1); xiid=rndnorm(0,1,N,1);
>> rAR(1)=riid(1); xAR(1)=xiid(1);
```

```

>> for i=2:N
>>   mr=a_r/(1-a_r)/nu*rAR(i-1);
>>   Nr=rndpois(mr);
>>   if Nr>0, E=rndexp(1,Nr,1); else E=0; end
>>   Kr=sum(E)/mr;
>>   rAR(i)=a_r*Kr*rAR(i-1)+(1-a_r)*riid(i);
>>   xAR(i)=a*xAR(i-1)+sqrt(1-a^2)*xiid(i);
>> end
>> yG=sy*xAR;
>> yL=sy*xAR.*(sqrt(riid));
>> yLAR=sy*xAR.*(sqrt(rAR));
>> subplot(3,1,1), plot(yG)
>> subplot(3,1,2), plot(yL)
>> subplot(3,1,3), plot(yLAR)

```

In the program the standard deviation of the topography  $Y_k$  is  $\sigma_y = 3.71$ , the shape parameter is  $\nu = 1.11$ , while the correlation parameters are  $a = 0.734$ ,  $a_r = 0.84$ . It corresponds to the parameters estimated from the measured topography in Figure 1. Using the MATLAB code, three topography models are simulated and plotted, namely Gaussian  $y_G$ , Laplace  $y_L$ , and Laplace with correlated gamma variances  $y_{LAR}$ , compare Figures 4 and 5.

## A.2 Simulation of Laplace road roughness models

The length of the simulated function will be 5 km and the sampling interval 5 cm. The following code can be used to compute the spectrum.

```

>> C=9.45e-6; ww=2;
>> Lp=5000; dx=0.05; NN=ceil(Lp/dx)+1; xx=(0:NN-1)'*dx;
>> w = pi/dx*linspace(-1,1,NN)'; dw=w(2)-w(1);
>> wL=2*pi/90; wR=2*pi/0.35;
>> C0=1/((1/wL.^(ww-1) - 1/wR.^(ww-1))/(ww-1));
>> sigma=sqrt(C/C0);
>> S=zeros(size(w));
>> indw=find(abs(w)>wL & abs(w)<wR);
>> S=zeros(NN,1); S(indw)=C/2*1./abs(w(indw)).^ww;
>> G=fftshift(sqrt(S))/sqrt(dx/dw/NN);
>> kernel=fftshift(real(ifft(G)));
>> figure, plot(w*dx/dw,kernel)

```

The kernel  $g(x)$  is introduced through its Fourier transform  $G(\Omega) = \mathcal{F}g(\Omega)$ . The standard deviation of the road is denoted by  $\sigma$ . If the load is Gaussian then  $\sigma$  is constant for whole length  $L_p$  and need to be estimated from the signal. We turn now to simulation of Gaussian and Laplace models.

### A.2.1 Gaussian model

First a Gaussian white noise process  $\text{InpG}$  is generated, then the road profile  $z_G$  is computed by means of FFT.

```

>> InpG=rndnorm(0,1,NN,1);
>> zG = sqrt(dx)*real(ifft(fft(InpG).*G));
>> figure, subplot(4,1,1), plot(xx,zG)

```

### A.2.2 Stationary Laplace model

For the LMA model, first, parameter  $\nu$  is computed for kurtosis, and then Laplace white noise `InpLMA` is evaluated, after which the road elevation `zLMA` is simulated:

```
>> nu=1;
>> rLMA=nu*randgam(1/nu,1,NN,1);
>> InpLMA=InpG.*sqrt(rLMA);
>> zLMA = sqrt(dx)*real(ifft(fft(InpLMA).*G));
>> subplot(4,1,2), plot(xx,zLMA)
```

### A.2.3 Non-stationary Laplace model

In the Laplace model it is assumed that the roughness is constant for a short segment of a road, here 100 metres. The Laplace shape parameter is here specified to  $\nu = 1$ , corresponding to a road profile kurtosis of 6. This determines the gamma distributed random variances `riid` and `rAR` for independent and AR cases, respectively. Then the modulation processes `mod` and `modAR` are evaluated and finally road elevations `zL` and `zLAR` are computed.

```
>> L=100; M=ceil(L/dx); NM=ceil(NN/M);
>> nu=1; a_r=0.9;
>> riid=nu*randgam(1/nu,1,1,NM);
>> rAR(1)=riid(1); % Gamma AR
>> for i=2:NM
>>   mr=a_r/(1-a_r)/nu*rAR(i-1);
>>   Nr=rndpois(mr);
>>   if Nr>0, E=rndexp(1,Nr,1); else E=0; end
>>   Kr=sum(E)/mr;
>>   rAR(i)=a_r*Kr*rAR(i-1)+(1-a_r)*riid(i);
>> end
>> mod=[]; modAR=[];
>> for j=1:NM;
>>   mod=[mod; sqrt(riid(j))*ones(M,1)];
>>   modAR=[modAR; sqrt(rAR(j))*ones(M,1)];
>> end
>> zL = sqrt(dx)*real(ifft(fft(InpG.*mod(1:NN)).*G));
>> zLAR = sqrt(dx)*real(ifft(fft(InpG.*modAR(1:NN)).*G));
>> subplot(4,1,3), plot(xx,zL)
>> subplot(4,1,4), plot(xx,zLAR)
```

Note that in the code the same sample of a Gaussian white noise `InpG` has been used to generate the Gaussian and non-stationary Laplace models of the road profile. This is done to facilitate visual comparison of the simulated records.

### A.2.4 Estimation of non-stationary Laplace model

Here we assume that from some database the sequence of IRI are available sampled also at 100 metres. The sequence is saved in a vector `IRI`.

```
>> Ci=(IRI/2.21).^2;
>> C=mean(Ci);
>> nu=var(Ci)/C^2;
```

The estimated parameters `C` and `nu` of the non-stationary Laplace model can then be used for simulating profiles. Note that if the simulated gamma variables `riid` are replaced by a corresponding vector of observed normalized variances

$\text{riid}=\text{Ci}/C$ , the same simulation code can be used for simulating a non-stationary Gaussian road profile.

### A.3 Simulation of bivariate Laplace road roughness model

A zero mean bivariate stationary Gaussian process is completely defined by its two power spectra and the normalized cross-spectrum. There are several means to simulate sample paths, and the algorithm proposed in (Shinozuka, 1971) is most commonly used. Here we present a method proposed in (Kozubowski et al., 2013) valid only for processes with real valued normalized cross-spectra  $K(\Omega)$ , see Eq. (32).

First introduce two kernels  $g_1(x)$  and  $g_2(x)$  by means of the Fourier transforms

$$\begin{aligned} (\mathcal{F}g_1)(\Omega) &= \sqrt{2\pi S_L(\Omega)} \cdot \left( \sqrt{1+K(\Omega)} + \sqrt{1-K(\Omega)} \right) / 2, \\ (\mathcal{F}g_2)(\Omega) &= \sqrt{2\pi S_R(\Omega)} \cdot \left( \sqrt{1+K(\Omega)} - \sqrt{1-K(\Omega)} \right) / 2. \end{aligned} \quad (40)$$

where  $S_L(\Omega)$  and  $S_R(\Omega)$  are the left and right spectra, respectively. Then two correlated Gaussian moving averages  $Z_L(x)$ ,  $Z_R(x)$  are given by

$$\begin{aligned} Z_L(x) &\approx \left( \sum g_1(x-x_i) Z_{1i} + \sum g_2(x-x_i) Z_{2i} \right) \sqrt{dx}, \\ Z_R(x) &\approx \left( \sum g_2(x-x_i) Z_{1i} + \sum g_1(x-x_i) Z_{2i} \right) \sqrt{dx} \end{aligned} \quad (41)$$

where  $Z_{1i}$ ,  $Z_{2i}$ 's are independent standard Gaussian random variables, with equality in limit as  $dx$  tends to zero.

Essentially, the Gaussian processes  $Z_L(x)$ ,  $Z_R(x)$  are obtained by filtering of sequences of independent standard Gaussian variables  $Z_{1i}$ ,  $Z_{2i}$ , which serve as two Gaussian noise sequences. The Laplace processes are constructed in a similar way, the difference is that now we allow  $Z_{1i}$ ,  $Z_{2i}$  to have variable gamma distributed variances, see Section 3.7 and Eq. (25). For completeness we give a MATLAB code to simulate the Laplace model.

```
>> C=9.45e-6; ww=2.5; b=1.15;
>> nu=0.33; a_r=0.41;
>> Lp=10000; L=100; dx=0.05;
>> NM=Lp/L; M=L/dx;
>> riid=nu*randgam(1/nu,1,NM,1);
>> rAR=riid;
>> for i=2:NM
>>   mr=a_r/(1-a_r)/nu*rAR(i-1);
>>   Nr=rdpois(mr);
>>   if Nr>0, E=rdexp(1,Nr,1); else E=0; end
>>   Kr=sum(E)/mr;
>>   rAR(i)=a_r*Kr*rAR(i-1)+(1-a_r)*riid(i);
>> end
>> Noise=[]; NoiseAR=[];
>> for i=1:NM
>>   Nois=rdnorm(0,1,2,M)';
>>   Noise=[Noise; sqrt(riid(i))*Nois];
>>   NoiseAR=[NoiseAR; sqrt(rAR(i))*Nois];
>> end
```

```

>> wL=0.011*2*pi; wR=2*pi*2.83;
>> C0=1/((1/wL.^(ww-1) - 1/wR.^(ww-1))/(ww-1));
>> sigma=sqrt(C/C0);
>> NN=NM*M;
>> w=pi/dx*linspace(-1,1,NN)'; dw=w(2)-w(1);
>> indw=find(abs(w)>wL & abs(w)<wR);
>> S=zeros(NN,1); S(indw)=C/2*1./abs(w(indw)).^ww;
>> SL=S; SR=S;
>> K=zeros(NN,1); K=exp(-b*abs(w));
>> G1=sqrt(2*pi*SL)/dx.*(sqrt(1+K)+sqrt(1-K))/2;
>> G2=sqrt(2*pi*SR)/dx.*(sqrt(1+K)-sqrt(1-K))/2;
>> G1=ifftshift(G1); G2=ifftshift(G2);
>> zLiid=real(ifft(fft(Noise(:,1)).*G1)+ifft(fft(Noise(:,2)).*G2))*sqrt(dx);
>> zRiid=real(ifft(fft(Noise(:,1)).*G2)+ifft(fft(Noise(:,2)).*G1))*sqrt(dx);
>> zLAR=real(ifft(fft(NoiseAR(:,1)).*G1)+ifft(fft(NoiseAR(:,2)).*G2))*sqrt(dx);
>> zRAR=real(ifft(fft(NoiseAR(:,1)).*G2)+ifft(fft(NoiseAR(:,2)).*G1))*sqrt(dx);
>> figure(1), plot((1:NN)*dx,[zLiid zRiid])
>> figure(2), plot((1:NN)*dx,[zLAR zRAR])

```

Using the code, 10 km long left and right profiles having ISO spectrum with waviness parameter  $w = 2.5$  sampled each 5 cm were simulated for independent and correlated factors  $r_j$ . Examples of simulated road profiles are shown in Figure 12.

#### A.4 Simulation of multi-axial correlated Laplace model

For readers convenience we present MATLAB code used to simulate standardized (zero mean variance one) multi-axial Laplace model having exponential spectrum introduced in Section 4.2. In (Kvanström et al., 2013) mathematical derivations leading to the algorithm are given.

Here we consider the standardized three dimensional load presented in Figure 14. We will simulate tri-axial load saved in  $X$  on interval  $[-T, T]$  with sample step  $dt$ . First the discretization step and related constants are set;

```

>> dt=0.001; T=120; N0=floor(T/2/dt); N=2*N0+1;
>> t=0.5*linspace(-T,T,N)';

```

We now evaluate kernels  $g$  and its transfer functions  $\mathcal{F}g(\omega)$ , see Eqs.(17) and (34),  $G_k$ . For this we define three exponential spectra (33) having parameters  $a$  and  $\sigma^2 = 1$ . Kurtosis of the loads are given in  $\kappa$  and the variances  $\nu$  of factors  $R_i$  are evaluated using (35) and saved in  $\nu$ ;

```

>> K=3; a=[0.012 0.009 0.015 ]; kappa=[11.4 9.4 20.1];
>> nu=0.42*(kappa-3).*a;
>> w=pi/dt*linspace(-1,1,N)'; dw=w(2)-w(1); S=[];
>> for i=1:K
>> S=[S 0.5*a(i)*exp(-a(i)*abs(w))];
>> end
>> Gk=ifftshift(sqrt(S))/sqrt(dt/dw/N);
>> g=fftshift(real(ifft(Gk)));

```

In the following script one defines the covariance structure of the Laplace model. The correlation matrices for jump sizes SIGMA (this defines sizes of transients) and the correlation of added Gaussian noise CG will be specified;

```

>> SIGMA = [1 0.5 0.9; 0.5 1 0.3; 0.9 0.3 1 ]; CG=eye(3);
>> [V,D] = eig(SIGMA); AJump=V*sqrt(D);
>> [V,D] = eig(CG); AGauss=V*sqrt(D);

```

Now we turn to the the simulation algorithm of the multi-axial Laplace model. The simulated load is given in the matrix  $X$ ; In the following script  $N_{\text{jmp}}$  defines number of transients, here we choose to be as many as the number of values of the load, i.e.  $N$ ;

```
>> X = zeros([N K]);
>> Njmp=N;
>> nu_min=min(nu);
>> G = exp(-nu_min*cumsum(rndexp(1,1,Njmp))/T);
>> W = sqrt(rndexp(1,1,Njmp));
>> Z = AJump*rndnorm(0,1,[K Njmp]);
>> dXG=sqrt(dt)*AGauss* rndnorm(0,1,[K N]);
>> indU=randperm(N);
>> for ii=1:K
>>     nui=nu(ii);
>>     p=sqrt(exp(-nui*Njmp/T));
>>     dLambda=zeros(1,N);
>>     dLambda(1,1:Njmp) = sqrt(nui)*Z(ii,:).*W.*G.^(nui/nu_min/2);
>>     dLambda=dLambda(indU)';
>>     dX = p*dXG(ii,:)+dLambda;
>>     X(:,ii) = real(ifft(Gk(:,ii).*fft(dX)));
>> end
>> figure, plot(t,X)
```

## List of abbreviations

AR	- Autoregressive
IRI	- International Roughness Index
ISO	- International Organization for Standardization
FFT	- Fast Fourier Transform
LMA	- Laplace Moving Average
PSD	- Power Spectral Density

## List of symbols and notation

$a$	- Autoregressive parameter for topography
$a_r$	- Autoregressive parameter for gamma AR-process
$b$	- scale parameter in exponential normalized cross-spectrum function
$C$	- roughness coefficient [ $\text{m}^3/\text{rad}$ ]
$E[X]$	- expectation of random variable $X$
$\mathcal{F}$	- Fourier transform
$g(x)$	- kernel for moving averages [ $\text{m}^{1/2}$ ]
$\Gamma(\cdot)$	- gamma function
$IRI$	- International Roughness Index [ $\text{mm}/\text{m}$ ]
$k$	- damage exponent
$K(\Omega)$	- normalized cross-spectrum
$L$	- length of road segments [ $\text{m}$ ]
$L_p$	- length of a road profile [ $\text{m}$ ]
$L_s$	- sampling distance for topography [ $\text{m}$ ]
$R_k$	- Gamma random variables
$r_j$	- factors describing variability of variances
$S(\Omega)$	- road profile model spectrum [ $\text{m}^3/\text{rad}$ ]
$\tilde{S}(\Omega)$	- normalized road profile model spectrum [ $\text{m}/\text{rad}$ ]
$S_{LR}(\Omega)$	- cross-spectrum [ $\text{m}^3/\text{rad}$ ]
$v$	- vehicle speed [ $\text{m}/\text{s}$ ]
$V[X]$	- variance of random variable $X$
$x$	- position of a vehicle [ $\text{m}$ ]
$w$	- waviness parameter in ISO spectrum
$X_k$	- Gaussian topography [%]
$Y_k$	- Laplace topography [%]
$Z(x)$	- road profile [ $\text{m}$ ]
$Z_L(x), Z_R(x)$	- left, right road profile [ $\text{m}$ ]
$\kappa$	- kurtosis of road profile
$\nu$	- scale parameter in gamma distribution
$\sigma$	- standard deviation of road profile [ $\text{m}$ ]
$\sigma_x, \sigma_y$	- standard deviation of topography [%]
$\omega$	- angular frequency [ $\text{rad}/\text{s}$ ]
$\Omega$	- spatial angular frequency [ $\text{rad}/\text{m}$ ]
$\Omega_L, \Omega_R$	- cutoff frequencies defining the ISO spectrum [ $\text{rad}/\text{m}$ ]



<http://journals.lub.lu.se/index.php/stat>



**LUND UNIVERSITY**  
School of Economics and Management

LUND UNIVERSITY  
SCHOOL OF ECONOMICS AND MANAGEMENT  
Department of Statistics  
Working Papers in Statistics No 2015  
Box 743  
220 07 Lund, Sweden